NASA
Technical
Paper
3084

AVSCOM
Technical
Report
91-B-004

April 1991

Determination of Flight Hardware Configuration of Energy-Absorbing Attenuator for Proposed Space Station Crew and Equipment Translation Aid Cart

Edwin L. Fasanella,
Karen E. Jackson,
Lisa E. Jones,
and John E. Teter, Jr.

US ARMY
AVIATION
SYSTEMS COMMAND
AVIATION R&T ACTIVITY

NASA

NASA Technical Paper 3084

AVSCOM Technical Report 91-B-004

1991

Determination of Flight Hardware Configuration of Energy-Absorbing Attenuator for Proposed Space Station Crew and Equipment Translation Aid Cart

Edwin L. Fasanella
Lockheed Engineering & Sciences Company
Hampton, Virginia

Karen E. Jackson
Aerostructures Directorate
USAARTA-AVSCOM
Langley Research Center
Hampton, Virginia

Lisa E. Jones and John E. Teter, Jr.
Langley Research Center
Hampton, Virginia

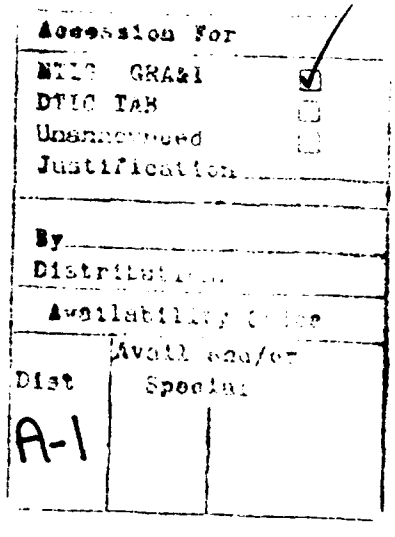

NASA
National Aeronautics and Space Administration
Office of Management
Scientific and Technical Information Division

Summary

The crew and equipment translation aid (CETA) cart is an advanced mobility concept designed to transport a maximum of two astronauts and additional equipment on the space station. As part of the design evaluation, an in-flight experiment consisting of a CETA cart attached to a 50-ft-long monorail will be operationally tested in the cargo bay of the Space Shuttle. Safety considerations require that an emergency stopping device be installed at the end of the monorail to bring the astronauts to a controlled stop in the event of a brake failure. A device incorporating a crushable honeycomb column as the energy-absorbing mechanism was designed for the emergency stop. Each honeycomb column was required to provide a nominal stopping force of 100 ± 15 lb and energy dissipation of at least 1650 in-lb for 16.5 in. of honeycomb stroke.

A series of impact tests was performed on various configurations of the honeycomb column to determine the design which satisfied the flight hardware requirements. A typical honeycomb column consisted of four 5.875-in-long segments of 75-psi honeycomb, separated by 0.125-in-thick washers. Specimens made of tube core or standard core honeycomb having aluminum, polyethylene, or Du Pont Teflon washers were tested. The impact tests were conducted in the small vertical drop tower located at the Langley Impact Dynamics Research Facility (IDRF). The honeycomb energy-absorbing column was supported inside a test sleeve which allowed radial clearance for the specimen to expand as it was compressed. The impact energy was provided by a mass car with an attached plunger which was dropped from a sufficient height to provide one half the equivalent kinetic energy of a 500-lb mass (astronaut plus equipment) moving at 6 ft/sec. A load platform under the test sleeve measured the stopping force of the honeycomb and a string potentiometer measured the vertical crush of the test specimen.

Twenty-six impact tests were performed. From load and displacement time histories for each test, load-displacement and energy-displacement curves were generated to evaluate the performance of the various honeycomb configurations. Based on the results of the impact tests, an energy-absorbing column constructed of standard core aluminum honeycomb with foil wrapping and Teflon washers met the design requirements and was chosen for the CETA flight experiment.

Introduction

The crew and equipment translation aid (CETA) cart is an advanced mobility concept designed to transport a maximum of two astronauts and additional equipment on the space station. The CETA hardware consists of an aluminum frame with wheels, called the CETA truck, which rides on a monorail onto which various carts can be attached. Three configurations have been developed which utilize manual, mechanical, and electrical propulsion systems. Figure 1 contains photographs from operational tests of each of the three types of carts. The tests were performed by astronauts in an underwater tank to simulate the weightlessness of space.

The simplest concept, the manual cart (fig. 1(a)), consists of a portable foot restraint (PFR) that is locked onto the CETA truck. The astronaut engages his foot in the PFR and manually pulls himself and the cart along the monorail. The braking system on the manual cart consists of pads which grip against the monorail when engaged by the astronaut through a flexible cable. The mechanical cart (fig. 1(b)) consists of the CETA truck and a second smaller cart, the tether shuttle. During operation, the astronaut straddles a frame which connects the CETA truck and tether shuttle together. The handle of the cart is pumped back and forth mechanically to provide locomotion. The electrical cart (fig. 1(c)) is driven by an electric motor which is powered by a hand-operated generator. The cart also uses a PFR to support the astronaut. Both the mechanical and electrical carts have primary braking systems which are more complex than the braking system on the manual cart but are also activated by the astronaut.

A flight experiment consisting of a CETA cart attached to a 50-ft-long monorail will be operationally tested in the Space Shuttle cargo bay to evaluate the performance of the designs. In the event of a primary brake failure for any of the CETA carts, a redundant, emergency braking system must be employed to safely stop the cart and astronaut. A device incorporating a crushable honeycomb column as the energy-dissipating mechanism was designed for the emergency stop.

In the CETA emergency braking system, the honeycomb tubes are contained inside a revolver mechanism (shown in fig. 2). Crushing is initiated when a metallic plunger on each side of the truck engages a honeycomb column through a slot in the revolver. The revolvers can be rotated 90° (fig. 2(b)) to provide specimens for two emergency stops. After two stops, the revolver can be taken apart and replacement columns inserted. Each honeycomb energy absorber was required to provide 100 lb of stopping force and minimum energy dissipation of 1650 in-lb for 16.5 in. of stroke, after which a hard stop is encountered.

Aluminum honeycomb has been used as an energy absorber for braking and decelerating numerous mechanical systems in a controlled manner (refs. 1 through 6). Some typical "one-shot" applications include: landing gear assemblies for surface landings of space probes (refs. 1 and 2), helicopter landing gears for crash landings (ref. 5), and aircraft seats for crashworthiness (ref. 6). The crushing stress of the aluminum honeycomb may be tailored for a wide variety of engineering applications by selecting the appropriate density, or cell size. For example, the crushing stress for 5052 aluminum alloy ranges from about 20 psi for densities of 1.5 lb/ft^3 to over 3200 psi for a density of 28 lb/ft^3 (ref. 4). The load response of honeycomb does exhibit some rate dependency. For a high velocity impact of 300 ft/sec, the dynamic crushing load can exceed the static crushing load by as much as 20 percent, depending on the ratio of cross-sectional area to perimeter (ref. 7) of the honeycomb configuration. For low velocity impacts, the static and dynamic crushing loads are nearly the same (within 5 percent) for low density honeycomb, as was typical of the loading conditions and type of honeycomb used for the CETA tests. Honeycomb is not usually recommended as an energy absorber if the required crush distance, or stroke, is greater than 1 m (ref. 7).

A variety of honeycomb configurations were fabricated to meet the CETA design requirements. Impact tests were conducted to evaluate the energy-absorbing responses of the honeycomb columns under loading conditions which simulate the impact of a CETA cart and astronaut following a primary brake failure. Experimental results from these impact tests are discussed and the various honeycomb designs are evaluated based on their energy-absorbing performance.

Experimental Program

Test Specimens

Twenty-six honeycomb specimens were dynamically tested. A description of the test parameters including the test number, specimen type, precrush orientation, drop mass, and drop height is given in table I. The 24-in-long specimens were made of four honeycomb segments each 1.18 in. in diameter by 5.875 in. long separated by washers (1.50 in. outside diameter, 0.25 in. inside diameter, and 0.125 in. thick), as shown in figure 3(a). Specimens were fabricated with washers made of polyethylene, aluminum, and Teflon to evaluate the effect of washer material on the energy-absorbing performance of the tube. Each of the 5.875-in. honeycomb segments was precrushed on one end to initiate crushing and to alleviate the initial force spike upon impact. The honeycomb segments were fabricated of 5052 aluminum with a 0.25-in. cell size and 0.001-in. wall thickness. Details of the honeycomb tube cross section are depicted in figure 3(b). The honeycomb crush strength was nominally 75 psi. Two specimens were fabricated of tube core honeycomb which is produced by alternately wrapping flat foil and corrugated aluminum around a mandrel until the required diameter is achieved. The remaining specimens were cut from standard core honeycomb and a foil wrap was glued onto the outside surface to close the outer cells of the honeycomb, as shown in figure 4. Two standard core honeycomb specimens were fabricated without the foil wrap and tested to determine the effect of the foil wrap on the crushing force. The segmented honeycomb-washer design was intended to minimize global buckling by reducing the effective column length by a factor of 4. In addition, the small precrush region contained within each honeycomb segment provided several locations to initiate crushing.

In addition to varying the washer material and type of honeycomb, three specimens were fabricated such that each 5.875-in. honeycomb segment crushed at a different force level. The force levels of the four segments for these "stepped" specimens were 70, 100, 130, and 160 lb. This design was intended to predispose the honeycomb segments to crush sequentially in order of crushing strength. Finally, in an attempt to prevent washer rotation, two specimens were fabricated and tested in which the nominally 0.125-in. washers were replaced with 0.5-in-thick Teflon washers or "plugs."

The following notation was used to designate each of the honeycomb specimens tested in this investigation:

TCA	tube core honeycomb, aluminum washers
TCP	tube core honeycomb, polyethylene washers
SCP	standard core, polyethylene washers
SCA	standard core, aluminum washers
SCPF	standard core, polyethylene washers, foil wrap
SCAF	standard core, aluminum washers, foil wrap
SCTF	standard core, Teflon washers, foil wrap
SCAFM	standard core, aluminum washers, foil wrap, modified (three middle washers are 0.5-in-thick Teflon)
SCTFS	standard core, Teflon washers, foil wrap, stepped crush

These designations will be used to identify specimens throughout the remainder of this report.

Test Apparatus

A schematic drawing of the drop tower used to perform the honeycomb impact tests is shown as figure 5. This drop tower has been used previously by other researchers to conduct impact tests on composite beams (refs. 8 through 10). Minor modifications were made to the drop tower to perform the honeycomb column crushing tests. The tower consists of four vertical steel rods which are 10 ft long and 1 in. in diameter. The rods are fastened at the bottom to a channel section fixed to the floor and at the top to a structural support beam of the building. A vertical steel rod (plunger) 30 in. long and 1 in. in diameter is attached to a slider which moves vertically along the two innermost rods through low friction bearings. The mass car translates along the two outermost rods on similar bearings and provides the impact energy needed to crush the honeycomb. The honeycomb energy absorber is placed vertically in a test sleeve, which simulates the support conditions provided by the flight hardware revolver. The lower end of the honeycomb housing fits inside an aluminum block which is fastened to a load platform attached to the lower channel section.

Initially, a test configuration was used in which the plunger-slider assembly rested on top of the honeycomb column which was placed inside the support housing. The mass car was raised to the desired drop height and released. Contact between the mass car and the slider occurred through spherical steel impact points. High acceleration spikes at impact were moderated by placing a section of hard rubber covered by small lead plates on the slider-mass-car impact point. This loading configuration required that the kinetic energy of the mass car be transferred upon impact to the stationary slider-plunger assembly and then into the honeycomb energy absorber. Some energy loss occurred during the inelastic collision between the mass car and the slider-plunger assembly. Additional weight was attached to the mass car to compensate for the reduction in impact energy. However, the complex impact scenario made precise calculation of the actual incident kinetic energy difficult, since the coefficient of restitution at impact was unknown. An alternate loading configuration was devised to simplify the mechanism of energy transfer.

In the second configuration, the slider and mass car were connected to form a single unit which was raised to the proper drop height and released to impact the honeycomb. The kinetic energy of the impactor was easily determined from the drop height and the weight of the combined mass car, slider, and plunger mechanism.

Instrumentation

Two channels of dynamic data were recorded for each test. Honeycomb crush was measured with a string-activated potentiometer displacement transducer (string potentiometer) attached to the plunger. The string potentiometer was extended as the honeycomb crushed under the impact of the dropped mass. Vertical load was obtained from four piezoelectric force transducers located between the load platform and the lower channel support. The four load cells are compact, sensitive, fast-response transducers for measuring dynamic and short-term static forces. Each load cell was rated for a maximum load of 5000 lb. A load cell was placed underneath each corner of the 4-in-square load platform. The output from each cell was summed electronically to obtain the total vertical force reacted through the load platform.

Data Acquisition

A personal-computer-based data acquisition system was used to collect two channels of data for each test. The two data channels were force from the load platform under the test sleeve and displacement (or honeycomb stroking distance) measured by the string-activated potentiometer. The analog signals for each channel were amplified and filtered prior to being digitized by a high-speed analog-to-digital data acquisition board. A 1-kHz low-pass filter which allows for quick transient response was used. The data acquisition board uses an industry standard 12-bit successive approximation, 8-μsec converter. The board is supported by a high-speed data-transfer utility program and by a slower spreadsheet data acquisition software package. The spreadsheet software was used to collect calibration data and initial readings for the load and plunger position prior to a test. Test data were collected at a rate of 8 kHz (4 kHz per channel) using the high-speed data-transfer software. Digitized test data were converted to engineering units using the calibration factors and zero readings obtained before the test. Because of the high sampling rate of the software, a large amount of data was generated for each test making the data files intractable. A data processing program was written to reduce the size of the data files by a factor of 4 (effective rate of 1000 samples/sec/channel). Spreadsheet software was used to calculate average velocity as a function of time, average force over the stroke, and the energy absorbed as a function of displacement.

Test Procedures

The original design criteria required that the emergency braking device bring an astronaut and cart configuration weighing 500 lb from a velocity of 6 ft/sec to a controlled stop in 16.5 in. with a desired constant stopping force of approximately 200 lb. For an astronaut and cart configurations having greater mass, the operating velocity must be reduced to remain within the safety margins provided by the emergency braking system. Two honeycomb energy-absorbing columns arranged in parallel and supported inside revolvers (shown in fig. 2(b)) were designed to meet the requirements for emergency stopping. The test conditions for a single honeycomb tube were based on one half of the kinetic-energy requirements for the complete system, that is, one half the kinetic energy to be dissipated is approximately 1650 in-lb based on a 500-lb mass moving at 6 ft/sec. The work to stroke one honeycomb column assuming 100 lb crush force for 16.5 in. is also 1650 in-lb.

The impact test conditions, listed in table I, were calculated based on the amount of incident energy required to crush a honeycomb column at least 16.5 in. with an expected honeycomb crush force of 100 lb. Ideally, if the tests had been performed with a horizontal apparatus such that the effects of gravity were eliminated, the actual impact test conditions of a 500-lb mass traveling at a velocity of 6 ft/sec could have been applied. Since the tests were performed in a vertical drop apparatus with gravity effects, a much smaller mass was required at a higher velocity to provide the correct incident energy (500 lb would crush the honeycomb statically). The drop height was held constant at 18 in. for most tests; this produced an incident velocity at honeycomb contact of approximately 10 ft/sec. The kinetic energy of the drop mass at honeycomb contact plus the change in potential energy of the drop weight from honeycomb contact to the end of honeycomb crush were equated to the external work performed by the honeycomb energy-absorbing tube to determine the required drop mass for a specified drop height.

As mentioned previously in the test apparatus section of this report, two test configurations were used. In the first configuration, the mass car was released from the drop height and impacted the slider-plunger assembly as it rested on top of the honeycomb column. Some energy loss was expected due to friction in the linear bearings as the slider translated along the vertical rods of the drop tower. In addition, a considerable amount of energy was lost in the inelastic collision of the mass car and slider-plunger assembly. Extra mass was added to the mass car to compensate for these energy losses. In the second configuration, the mass car and slider-plunger assembly were fastened together to eliminate the inelastic collision effect. Some additional mass was still necessary to compensate for frictional losses in this setup.

A single test was performed in which a standard core specimen with foil wrap and Teflon washers (SCTF) was placed inside the actual CETA flight test hardware (revolver) and impacted. This test was conducted to ensure that the test sleeve simulated the support conditions of the revolver adequately. The first test configuration in which the slider-plunger assembly rested on the honeycomb column was used to reduce the risk of damage to the flight hardware.

The test procedure consisted of the following steps. The honeycomb specimen was inserted into the support sleeve in the desired orientation, either precrush up or down. An appropriate amount of lead weight was attached to the mass car to achieve the desired drop mass as specified in the test conditions (table I). The mass car was raised to the correct drop height and secured in position by a release hook. Instrumentation settings were verified and calibration and zero signals were collected with the data acquisition system. At time zero, the mass car was released and data from the load platform and string potentiometer were collected. Following the test, the crushed honeycomb column was carefully removed from the sleeve and examined for damage mechanisms and uniformity of crush.

Results and Discussion

Experimental Data

Plots of load versus time, load versus displacement, and energy versus displacement for all 26 impact tests are presented in figures 6 through 31. A numerical integration (trapezoidal rule) was performed on the load-displacement data to obtain the energy required to stroke the honeycomb. The criteria called for a minimum of 1650 in-lb of energy to be dissipated over the 16.5 in. of stroke. The average honeycomb force is computed by dividing the energy absorbed by the stroke distance. The data beyond a stroke of 16.5 in. are not meaningful because the honeycomb in the actual CETA hardware can only stroke 16.5 in. before a hard stop (metal-to-metal contact) occurs. In the experimental tests, the maximum possible stroke before the honeycomb becomes "solid" is slightly over 20 in. Table II lists values of total energy absorbed and average crushing load as calculated from the raw data for each impact test. Posttest photographs of the honeycomb specimens are shown in figures 32 through 38.

The first test configuration in which the mass car impacted the slider-plunger assembly as it rested on the honeycomb column was used in the first six tests and in test 17 of the flight hardware revolver. The second test configuration in which the mass car and slider-plunger assembly were fixed together was used in the remaining tests. Ideally, if the incident kinetic energy impacting the honeycomb is the same for the two configurations, then the response of the honeycomb tubes should be independent of the test method.

Tube Core Specimens

Results for the two tube core specimens, one having aluminum washers (TCA) and one having polyethylene washers (TCP), are presented in figures 6 and 7, respectively. Both tube core specimens crushed approximately 20 in. under nearly identical impact test conditions. Although the force level for the TCA specimen remained fairly constant, the force for the TCP specimen dropped and rose significantly between 5 and 10 in. of stroke. This erratic load response can be attributed to either local buckling and/or rotation of the washers. The washer rotation phenomenon is described more fully in the section "Testing Anomalies." Figure 32 contains a photograph of the TCA and TCP posttest specimens. The photograph indicates that the washers of the TCP specimen rotated severely, and this prevented the uniform crushing response exhibited by the TCA specimen. The average honeycomb force for each of the tube core specimens given in table II is approximately 70 lb. This value is below the nominal 100 lb needed to satisfy the design requirements; consequently, no further testing of tube core specimens was performed.

Standard Core Specimens

In the initial phase of testing, four standard core specimens were tested to identify the effects of washer material and foil wrapping on energy-absorbing performance. As shown in figure 8, the SCP specimen had a nearly constant crushing force of approximately 94 lb (disregarding noise and high frequency vibrations). However, the honeycomb only stroked 11.9 in. The photograph of figure 32 shows that the center segments of the SCP specimen exhibited little or no crushing. This finding implied that the weight on the mass car was too low at 50 lb to provide sufficient impact energy to completely crush the SCP specimen. Consequently, the weight of the mass car was increased to 60.1 lb for the subsequent tests. The additional weight provided a 20-percent increase in incident kinetic energy. Data plots from tests on SCA, SCPF, and SCAF honeycomb specimens are given in figures 9, 10, and 11, respectively. Although the average force exhibited by these specimens was between 96 and 97 lb (table II), only the SCA specimen had a force level which remained nearly constant with stroke (fig. 9). The SCA specimen, shown in figure 32, exhibited uniform crushing, except for a small portion of the center segment which remained uncrushed. The more erratic load responses of the SCPF specimen (fig. 10) and the SCAF specimen (fig. 11) are attributed to rotation of the washers. As shown in figure 32, the second and third internal washers (from the top) of the SCPF specimen rotated. For the SCAF specimen, the third internal washer from the top rotated at a stroke of 4 in. and a low force level of 25 lb. The SCAF specimen eventually crushed the entire 16.5 in., but the force level increased to a high value of 150 lb near the end of the stroke. Consequently, although the three standard core specimens which were tested with the higher weight stroked over 16.5 in. and the average force was nearly 100 lb, only the SCA specimen behaved as required.

Foil wrap, aluminum washer specimens. In the next series of tests (7 through 12), six specimens of standard core aluminum with a foil wrap and aluminum washers were impacted under the test conditions stated in table I. The data are shown in figures 12 through 17 and the posttest photographs of the specimens are shown in figure 33. These tests were performed in the second configuration with the mass car attached to the slider-plunger assembly.

The SCAF specimen of test 7 exhibited a nearly constant honeycomb force of 111 lb, as shown in figure 12, but crushed only 10.7 in. The posttest specimen (fig. 33) shows that the two lower segments of the honeycomb column are uncrushed. The low amount of honeycomb stroke indicates that the incident kinetic energy for the test was insufficient. The total weight for this test using the second configuration was 55.5 lb. The weight was subsequently increased to 67.2 lb for the next five tests in this series. As in the first configuration, the additional mass produced a 20-percent increase in incident kinetic energy. The SCAF specimen of test 8, which was impacted with the increased mass, exhibited poor crushing response because the aluminum washers rotated and jammed inside the test sleeve. Load-deflection results from this test, plotted in figure 13, show a stepped force response with the force at the end of the 10.8-in. stroke reaching 500 lb. As shown in figure 33, the first internal washer of the SCAF specimen rotated and contacted the support sleeve. Galling of the washer was evident from posttest examination. The average force of 147 lb from this

test exceeded the design requirements. It is noted that the SCAF specimens of tests 7 and 8 were oriented with the precrush regions in an upward position. This orientation yielded unsatisfactory results because the crush zone is required to displace further than when the precrush is oriented downward. Thus, more friction is generated and there is a greater chance of uneven crushing. Results for the SCAF specimen (test 9) are shown in figure 14. This specimen had the maximum stroke (18 in.) for all the SCAF specimens tested. The average force was 108 lb and the force level was constant until approximately 13 in. of stroke. Washer rotation, as shown in figure 33, and transverse crushing of the tube resulted in a severe drop in the load, but since the washer did not jam in the sleeve, the force level did not rise to as high a level as in the previous test.

Load-deflection plots for the next SCAF specimens (tests 10 and 11) are shown in figures 15 and 16, respectively. In both specimens the force near the end of the stroke rose to approximately 200 lb, even though photographs of the posttest SCAF specimens, shown in figure 33, indicate that uniform crushing occurred. Results for the final SCAF specimen (test 12), shown in figure 17, indicate that this was a successful test since the average force was 112 lb and the honeycomb stroked 16.4 in. at a constant force level. However, the second internal washer from the top of the SCAF specimen rotated approximately 60°, as shown in figure 33. In general, results from tests on several SCAF honeycomb columns indicate that aluminum washers are not desirable, since seizure of a washer in the sleeve might produce an unacceptably high load spike.

Foil wrap, Teflon washer specimens. In the next series of tests (13 through 16), four specimens of standard core honeycomb with foil wrap and Teflon washers were impacted. The second test configuration with a total mass of 67.2 lb was used, as indicated in table I. The posttest photographs of the four specimens are shown in figure 34 and the test data are shown in figures 18 through 21. The performance of the first SCTF specimen (test 13) was excellent with an average force of 107 lb over the total stroke of 18.4 in. Crushing occurred at a nearly constant force level. The average load over 16.5 in. was 105 lb. In figure 34, the posttest SCTF specimen of test 13 shows uniform crushing with no washer rotation. Results from the SCTF specimen of test 14 were similar to those of test 13 except that the average force was slightly higher at 112 lb. However, rotation of the washers occurred in the SCTF specimens of tests 15 and 16, as shown in figure 34, which is a photograph of the posttest specimens. The second internal washer of the SCTF specimen (test 15) rotated 90° and the honeycomb jammed in the sleeve to raise the average force to 127 lb. The stroke for this test was only 13.9 in. which was the smallest stroke for any of the SCTF specimens tested in this series. In test 16, washer rotation caused the force to drop sufficiently so that the average force was 98.7 lb over 16.5 in. The SCTF column of test 16 crushed completely with 19.7 in. of stroke. Although washer rotation and nonuniform crushing occurred in two of the four SCTF specimens, three of these specimens met the design requirements. Only the SCTF specimen of test 15 did not meet the requirements.

Foil wrap, Teflon washer specimen in revolver. An SCTF honeycomb specimen was impacted in the flight hardware revolver (fig. 2) in test 17 to verify that the test sleeve simulated the actual in-flight conditions properly. Since extra caution was needed for this test to ensure that the revolver was undamaged, the first test configuration in which the plunger rested on the honeycomb was used. The mass and drop height were similar to the conditions used in the initial tests. (See table I.) Results for the SCTF specimen tested in the flight hardware are given in figure 22 and table II. The stroke of 15.4 in. was slightly lower than anticipated (16.5 in. of stroke was desired). The average force of 101 lb met the design requirement; however, the force increased to a high level of 140 lb over the last inch of specimen stroke. The SCTF specimen of test 17 exhibited uniform crushing, as shown in figure 35.

Foil wrap, Teflon plug (modified) specimens. The next series of tests (18 and 19) were conducted on modified specimens made of standard core honeycomb wrapped in foil with aluminum outer washers. However, the internal standard 0.125-in-thick washers were replaced with three 0.5-in-thick Teflon plugs. This modification was made in an attempt to prevent washer rotation. The second test configuration was used with a total mass of 67.2 lb. The data from the two tests are shown in figures 23 and 24. As indicated in table II, the average force for both SCAFM specimens was higher than the design limit, 121 lb for test 18 and 136 lb for test 19. Correspondingly, the stroke for both the SCAFM specimens was under the 16.5-in. design requirement. Although the thick washers could not rotate, buckling of the second honeycomb segment of the SCAFM specimen (test 19) did occur, as shown in figure 36. Since washer rotation was prevented, the force in the specimen following formation of the buckle tended to jam the honeycomb in the sleeve. The resultant force was higher than that observed for specimens having standard

washers since higher frictional forces were generated between the plugs and the test sleeve. This concept was abandoned and no further testing was performed.

Foil wrap, Teflon washer, stepped strength specimens. The effect of using different strength honeycomb segments in the construction of the column was next studied (tests 20–22). Crushing force levels of the four segments for these stepped specimens (SCTFS) were 70, 100, 130, and 160 lb. The total drop mass was increased from 67.2 to 76.2 lb for these tests since higher incident energy was anticipated to fully crush these specimens. The drop height was a nominal 18 in. as in all the previous tests. Figures 25 through 27 contain plots of the data for these tests, and figure 37 is a photograph of the posttest specimens. All specimens crushed over 16.5 in. and uniform crushing was observed. However, the average force exhibited by the SCTFS specimens varied from 126 lb to 134 lb, which exceeded the design requirement force level. As is evident in figure 37, the weaker segments of the honeycomb column tended to crush completely, whereas the highest strength segment crushed very little.

Foil wrap, Teflon washer specimens, lower velocity. Based on test results from the various honeycomb column configurations, the SCTF specimens exhibited the best overall performance. Consequently, the SCTF configuration was chosen for further testing to obtain data for lower velocity impact test conditions. Four additional tests (23–26) were performed. The amount of drop mass was increased from the amount used in the previous SCTF tests to 76.2 lb; however, the drop height was reduced from 18 in. to 12.75 in. to lower the initial impact velocity to approximately 8 ft/sec. The data from these four tests are shown in figures 28 through 31 and the posttest photographs of the specimens are shown in figure 38. The average crushing load of the SCTF specimens ranged from 112 lb to 116.5 lb. The stroke varied from 15.8 in. to 17.2 in. Figure 38 illustrates that the two SCTF specimens with minor or no washer rotation (tests 23 and 26) showed the most uniform crushing behavior, whereas the specimens with significant washer rotation (tests 24 and 25) had poorer crushing performance.

Testing Anomalies

The results involving nonuniform crushing of the honeycomb tubes were traced to problems associated with misalignment of the washers along a common centerline and concentricity of the honeycomb sections with the washers. Some specimens were difficult to insert into the test sleeve due to this misalignment. In the most severe case, insertion of the honeycomb specimen caused a side force to be generated. A schematic drawing showing a mechanism that explains washer rotation is shown in figure 39. The washer and sleeve diameter is approximately 1.5 in., whereas the honeycomb diameter is only 1.18 in. If the centerlines of two adjacent honeycomb segments having a single washer between them are misaligned with the sleeve centerline, then a moment can develop that causes rotation of the washer, as illustrated in figure 39. Since misalignment of the honeycomb sections can result in poor crushing performance, improved quality control can be used to identify and reject specimens that contain these construction defects.

The diameter of the honeycomb tubes (1.18 in.) was chosen to obtain a crushing force of approximately 100 lb given a nominal 75-psi strength honeycomb. The inside diameter of the CETA flight hardware revolver and the test sleeve which was used to simulate the revolver for the impact testing was 1.50 in. This mismatch in diameters between the honeycomb and its support housing would provide clearance to allow the honeycomb to expand as it crushed. However, it is apparent that the clearance between the honeycomb tube and the supporting sleeve was excessive and should be minimized to ensure that the column is fully supported along its sides. If the diameters of the honeycomb column and the washers were the same, alignment problems could be reduced in manufacturing of the honeycomb tubes.

The washer material was found to be important. When aluminum was used, the aluminum-to-aluminum contact caused galling of the test sleeve to occur which can generate large frictional forces. Teflon washers provided lower sliding friction than the aluminum washers and, in addition, did not gall the aluminum test sleeve.

Flight Hardware Determination

The design requirements for an emergency braking system on the CETA cart required that a single honeycomb tube dissipate 1650 in-lb of energy with a stopping force of 100 ± 15 lb over 16.5 in. of stroke. Based on the results of impact tests, a honeycomb energy-absorbing column made from standard core aluminum honeycomb with a foil wrap and Teflon washers (SCTF) most consistently met the design requirements.

The SCTF specimens performed well for both velocity conditions tested (8 and 10 ft/sec). The average load for maximum stroke (table II) for the nine SCTF tests tended to be above 100 lb; however, only

one SCTF specimen (test 15) exceeded the maximum design requirement of 115 lb by a significant amount. That specimen showed severe washer rotation and nonuniform crushing behavior. The observed crushing of the SCTF specimens, even with some washer rotation, was nearly uniform. Some specimens did not stroke the entire 16.5 in.; however, generally the total specimen crush was close to the requirement. The incident energy for specimens that did not stroke 16.5 in. may have been slightly low due to energy losses in the drop rig.

Summary of Results

An experimental program was conducted to evaluate the crushing response of honeycomb tubes used as energy absorbers for an emergency braking system on the CETA cart. The design requirements specified that a single honeycomb tube provide a nominal stopping force of 100 lb and energy dissipation of at least 1650 in-lb for 16.5 in. of stroke.

The 24-in-long energy-absorbing tubes were fabricated by alternating thin washers and segments of aluminum honeycomb which were bonded together to form a single unit. Honeycomb tubes were designed with two different types of aluminum honeycomb (tube core and standard core) and three different washer materials (aluminum, polyethylene, and Teflon). Additionally, some specimens were wrapped with a thin aluminum foil on the outer circumference. To alleviate poor crushing performance caused by washer rotation, several specimens were fabricated with thicker Teflon plugs instead of thin washers. Also, a configuration was designed in which each honeycomb segment of the tube had a different crushing load level. In all, 26 impact tests were performed to evaluate the energy-absorbing responses of the honeycomb columns under loading conditions which simulate the impact of a CETA cart and astronaut following a primary brake failure.

Important results from this investigation are as follows:

1. The tube core aluminum honeycomb specimens which were tested in this investigation exhibited an average force which was too low to meet the design requirement.

2. Results for standard core honeycomb specimens with aluminum washers indicated that high load spikes may be produced if nonuniform crushing occurs and the washers rotate and seize inside the support housing.

3. In general, Teflon washers provided lower sliding friction than the aluminum washers, and honeycomb specimens fabricated with Teflon washers had better crushing performance. In addition, Teflon washers did not gall the aluminum test sleeve if rotation of the washers occurred during a test.

4. Average force and stroke distance were similar for specimens tested in the CETA flight hardware (revolver) and the test sleeve. This result implies that the test sleeve adequately simulated test conditions in the actual flight hardware.

5. Modified specimens in which the thin internal washers were replaced with 0.5-in-thick Teflon plugs exhibited an average crushing load which exceeded the design criterion. The Teflon plugs did not rotate; however, specimen buckling did occur.

6. The average force for the stepped strength honeycomb specimens was higher than the design limit, even though uniform crushing was observed.

7. Based on the results of this experimental program, a standard core honeycomb tube with a foil wrap and Teflon washers best satisfied the design requirements. This specimen was recommended for use as the energy-absorbing column for the emergency braking system on the CETA cart.

NASA Langley Research Center
Hampton, VA 23665-5225
February 22, 1991

References

1. Mackrill, F. P.: *Energy Absorbing Characteristics of Crushable Aluminum Structures in a Space Environment.* NASA CR-65096, 1965.

2. McCarty, John Locke; and Carden, Huey D.: *Experimental Study of Vertical Impacts of an LM-Type Landing Gear Assembly Under Simulated Lunar Gravity.* NASA TN D-4711, 1968.

3. Kindervater, C.: Quasi-Static and Dynamic Crushing of Energy Absorbing Materials and Structural Components With the Aim of Improving Helicopter Crashworthiness. *Seventh European Rotorcraft and Powered Lift Aircraft Forum*, Deutsche Gesellschaft für Luft- und Raumfahrt e.V. Goethestr. (Germany), 1981, pp. 66-1–66-25.

4. Coppa, Anthony P.: New Ways To Soften Shock. *Mach. Design*, vol. 40, no. 8, Mar. 28, 1968, pp. 130–140.

5. Rich, M. J.: Vulnerability and Crashworthiness in the Design of Rotary Wing Vehicle Structures. SAE Paper 680673, Oct. 1968.

6. Desjardins, S. P.; Zimmermann, Richard E.; Bolukbasi, Akif O.; and Merritt, Norman A.: *Aircraft Crash Survival Design Guide. Volume IV Aircraft Seats, Restraints, Litters, and Cockpit/Cabin Delethalization.* USAAVSCOM TR 89-D-22D, U.S. Army, Dec. 1989. (Available from DTIC as AD A218 437.)

7. Kirk, J. A.: Mechanical Energy Absorbers and Aluminum Honeycomb. *Trans. ASME, J. Mech. Design*, vol. 104, no. 3, July 1982, pp. 671–674.

8. Derian, E. J.; and Hyer, M. W.: *Large Deformation Dynamic Bending of Composite Beams.* NASA CR-4006, 1986.

9. Sensmeier, Mark D.; Griffin, O. Hayden, Jr.; and Johnson, Eric R.: *Static and Dynamic Large Deflection Flexural Response of Graphite-Epoxy Beams.* NASA CR-4118, 1988.

10. Jackson, Karen E.: *Scaling Effects in the Static and Dynamic Response of Graphite-Epoxy Beam-Columns.* NASA TM-102697, AVSCOM TR-90-B-006, 1990.

Table I. Test Parameters

Test	Specimen type[a]	Mass car, lb	Slider and plunger, lb	Drop height, in.	Precrush orientation
1	TCA	50.0	15	18.0	Down
2	TCP	50.0	15	17.8	Down
3	SCP	50.0	15	17.9	Down
4	SCA	60.1	15	17.8	Down
5	SCPF	60.1	15	17.6	Down
6	SCAF	60.1	15	17.7	Down
7	SCAF	55.5	[b]	18.3	Up
8	SCAF	67.2	[b]	18.1	Up
9	SCAF	67.2	[b]	18.0	Down
10	SCAF	67.2	[b]	18.0	Down
11	SCAF	67.2	[b]	18.0	Down
12	SCAF	67.2	[b]	18.0	Down
13	SCTF	67.2	[b]	18.5	Down
14	SCTF	67.2	[b]	18.0	Down
15	SCTF	67.2	[b]	17.8	Down
16	SCTF	67.2	[b]	17.8	Down
17	SCTF	60.1	15	18.8	Down
18	SCAFM	67.2	[b]	18.3	Down
19	SCAFM	67.2	[b]	18.0	Down
20	SCTFS	76.2	[b]	18.5	Down
21	SCTFS	76.2	[b]	18.5	Down
22	SCTFS	76.2	[b]	18.0	Down
23	SCTF	76.2	[b]	12.3	Down
24	SCTF	76.2	[b]	12.6	Down
25	SCTF	76.2	[b]	12.9	Down
26	SCTF	76.2	[b]	12.8	Down

[a]TCA: tube core, aluminum washers; TCP: tube core, polyethylene washers; SCP: standard core, polyethylene washers; SCA: standard core, aluminum washers; SCPF: standard core, polyethylene washers, foil wrap; SCAF: standard core, aluminum washers, foil wrap; SCTF: standard core, Teflon washers, foil wrap; SCAFM: standard core, aluminum washers, foil wrap, modified (replaced three middle washers with 0.5-in-thick Teflon washers); SCTFS: standard core, Teflon washers, foil wrap, stepped crush.

[b]Configuration with mass car, slider, and plunger rigidly connected.

Table II. Test Results

Test	Specimen type[a]	Maximum stroke, in.	Total energy absorbed, in-lb	Average load for maximum stroke, lb	Energy absorbed for 16.5-in. stroke, in-lb	Average load for 16.5-in. stroke, lb
1	TCA	19.7	1440	73.1	1163	70.5
2	TCP	20.9	1461	69.9	964	58.4
3	SCP	11.9	1120	94.1	(b)	(b)
4	SCA	16.5	1597	96.8	1597	96.8
5	SCPF	17.0	1637	96.3	1597	96.8
6	SCAF	16.6	1609	96.9	1586	96.1
7	SCAF	10.7	1194	111.6	(b)	(b)
8	SCAF	10.8	1584	146.7	(b)	(b)
9	SCAF	18.0	1946	108.1	1772	107.4
10	SCAF	15.7	1852	118.0	(b)	(b)
11	SCAF	15.9	1852	116.5	(b)	(b)
12	SCAF	16.4	1844	112.4	(b)	(b)
13	SCTF	18.4	1961	106.6	1732	105.0
14	SCTF	17.2	1944	113.0	1853	112.3
15	SCTF	13.9	1765	127.0	1765	127.0
16	SCTF	19.7	2059	104.5	1628	98.7
17	SCTF	15.4	1568	101.8	(b)	(b)
18	SCAFM	15.4	1866	121.2	(b)	(b)
19	SCAFM	12.7	1726	135.9	(b)	(b)
20	SCTFS	18.3	2299	125.6	2003	121.4
21	SCTFS	16.8	2244	133.6	2184	132.4
22	SCTFS	17.6	2277	129.4	2093	126.8
23	SCTF	16.5	1859	112.7	1859	112.7
24	SCTF	15.8	1840	116.5	(b)	(b)
25	SCTF	15.8	1829	115.8	(b)	(b)
26	SCTF	17.2	1927	112.0	1836	111.3

[a]TCA: tube core, aluminum washers; TCP: tube core, polyethylene washers; SCP: standard core, polyethylene washers; SCA: standard core, aluminum washers; SCPF: standard core, polyethylene washers, foil wrap; SCAF: standard core, aluminum washers, foil wrap; SCTF: standard core, Teflon washers, foil wrap; SCAFM: standard core, aluminum washers, foil wrap, modified (replaced three middle washers with 0.5-in-thick Teflon washers); SCTFS: standard core, Teflon washers, foil wrap, stepped crush.

[b]Did not stroke 16.5 in.

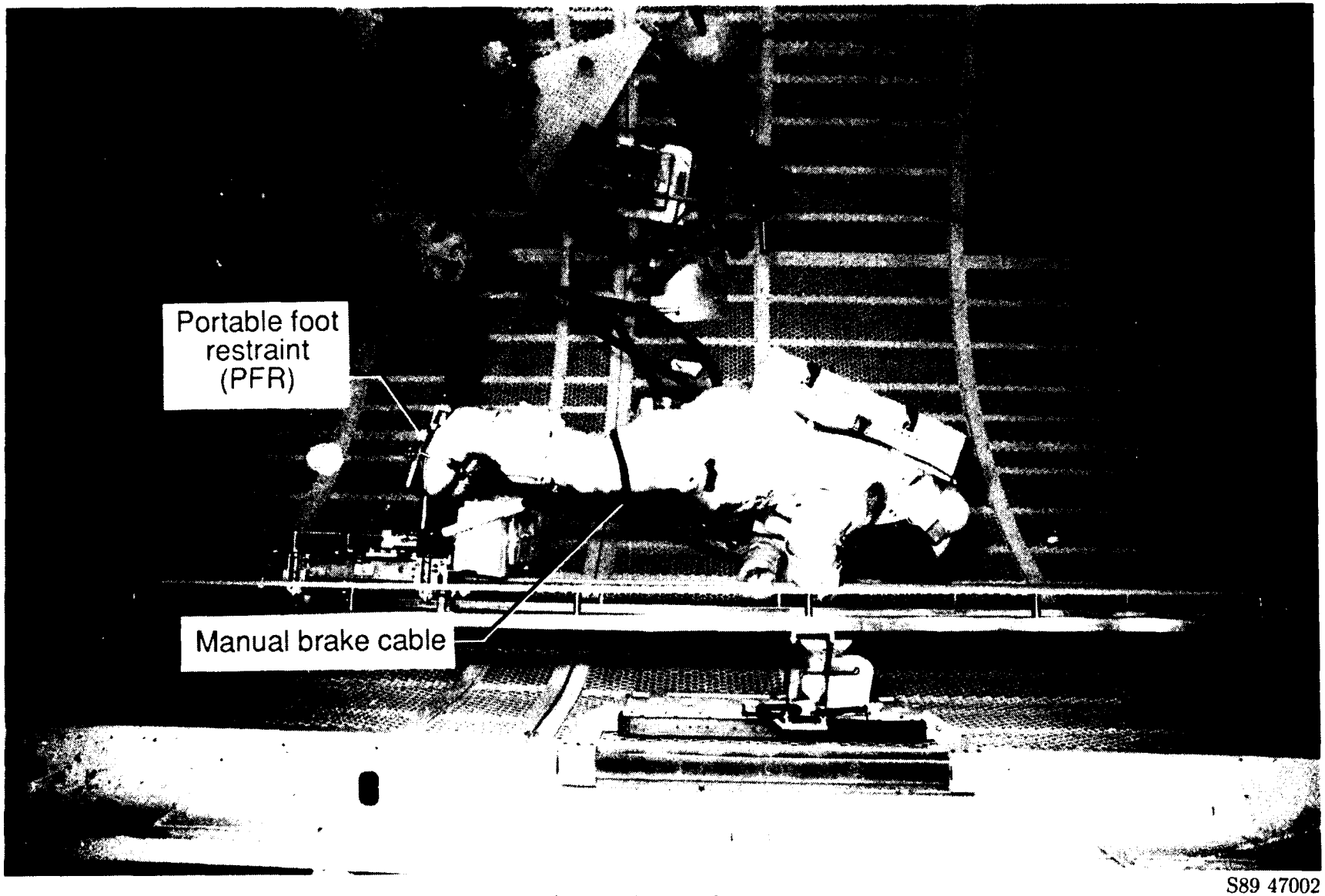

(a) CETA manual cart.

Figure 1. CETA carts during operational underwater tests.

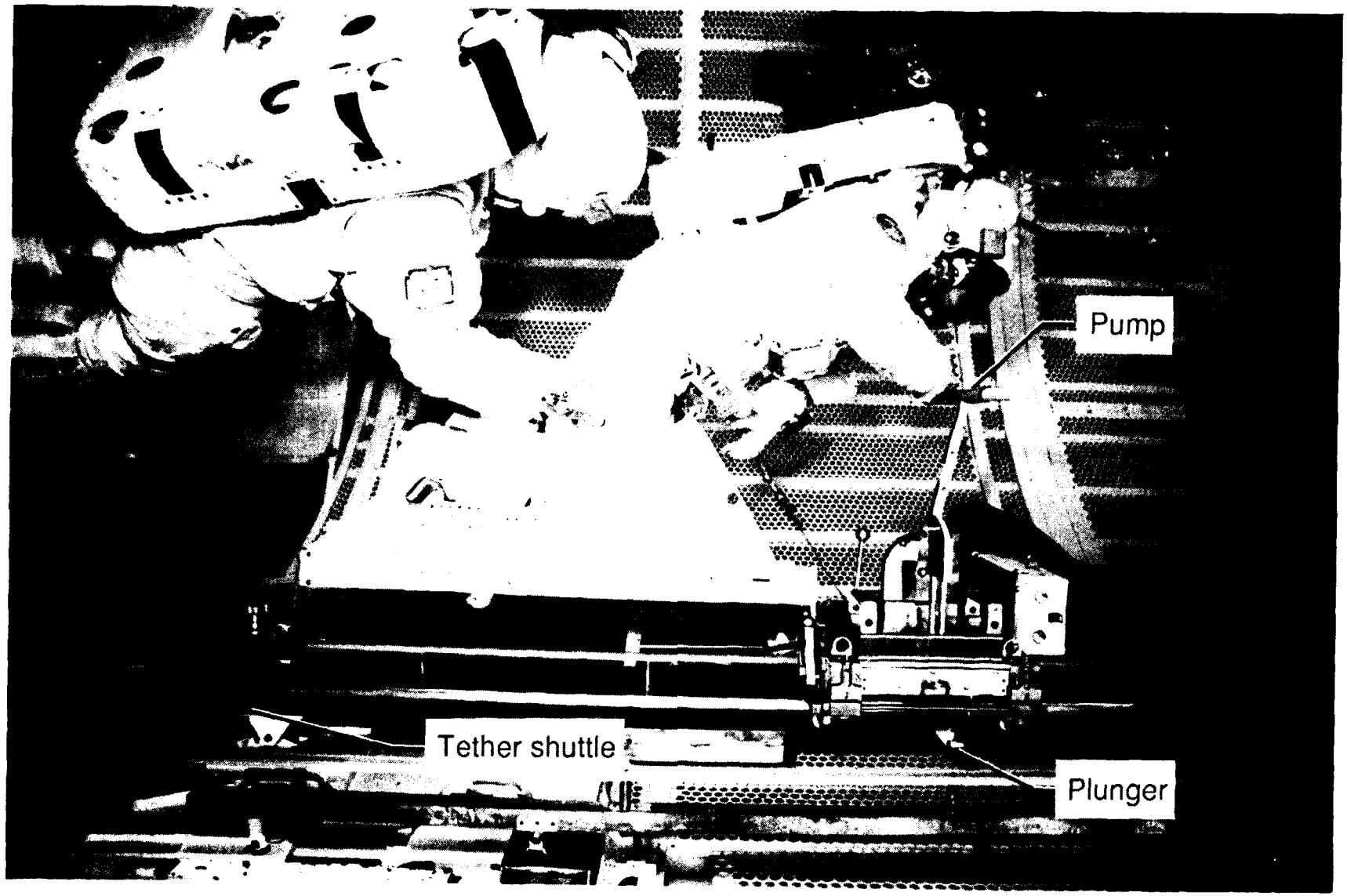

S89 48646

(b) CETA mechanical cart.

Figure 1. Continued.

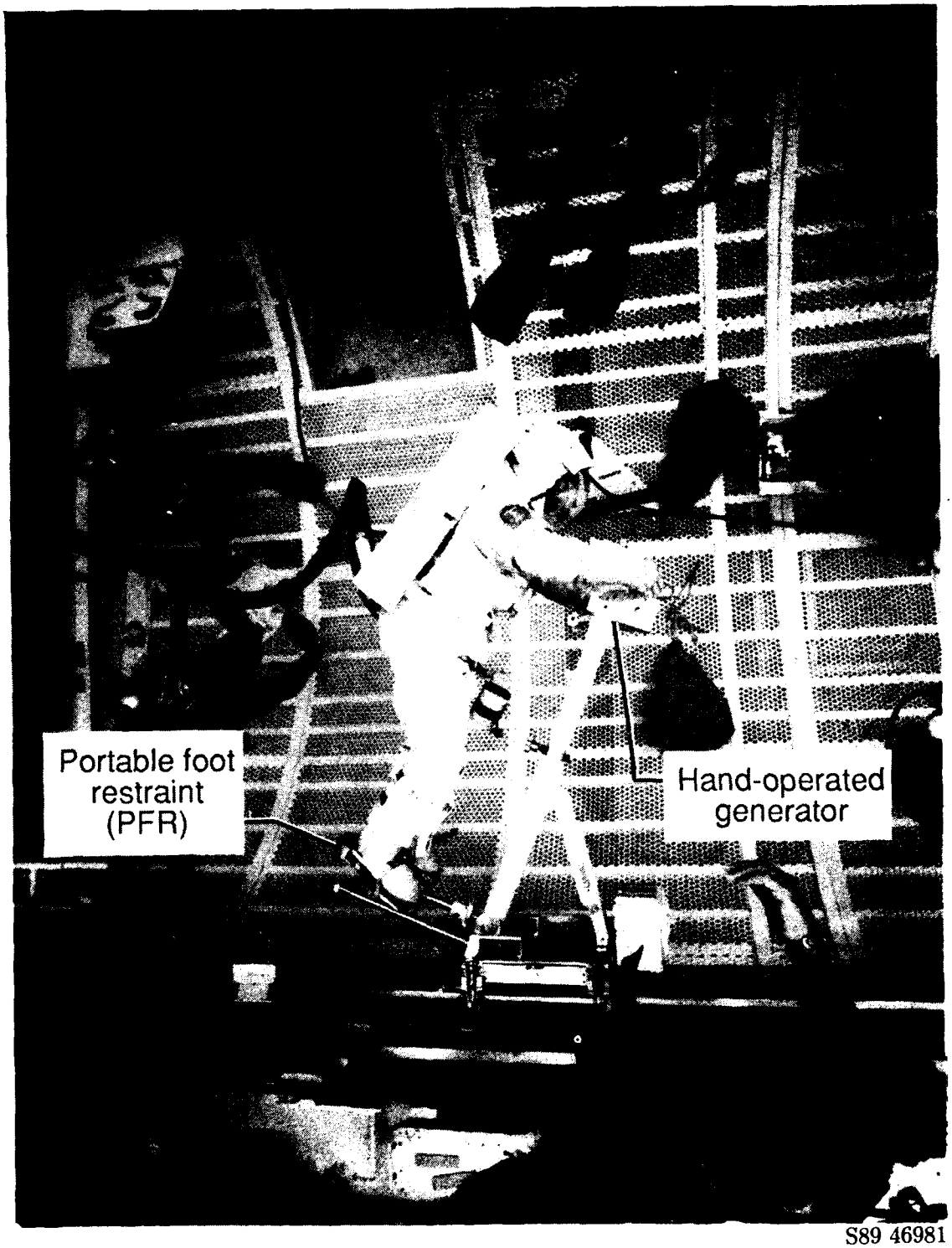

(c) CETA electrical cart.

Figure 1. Concluded.

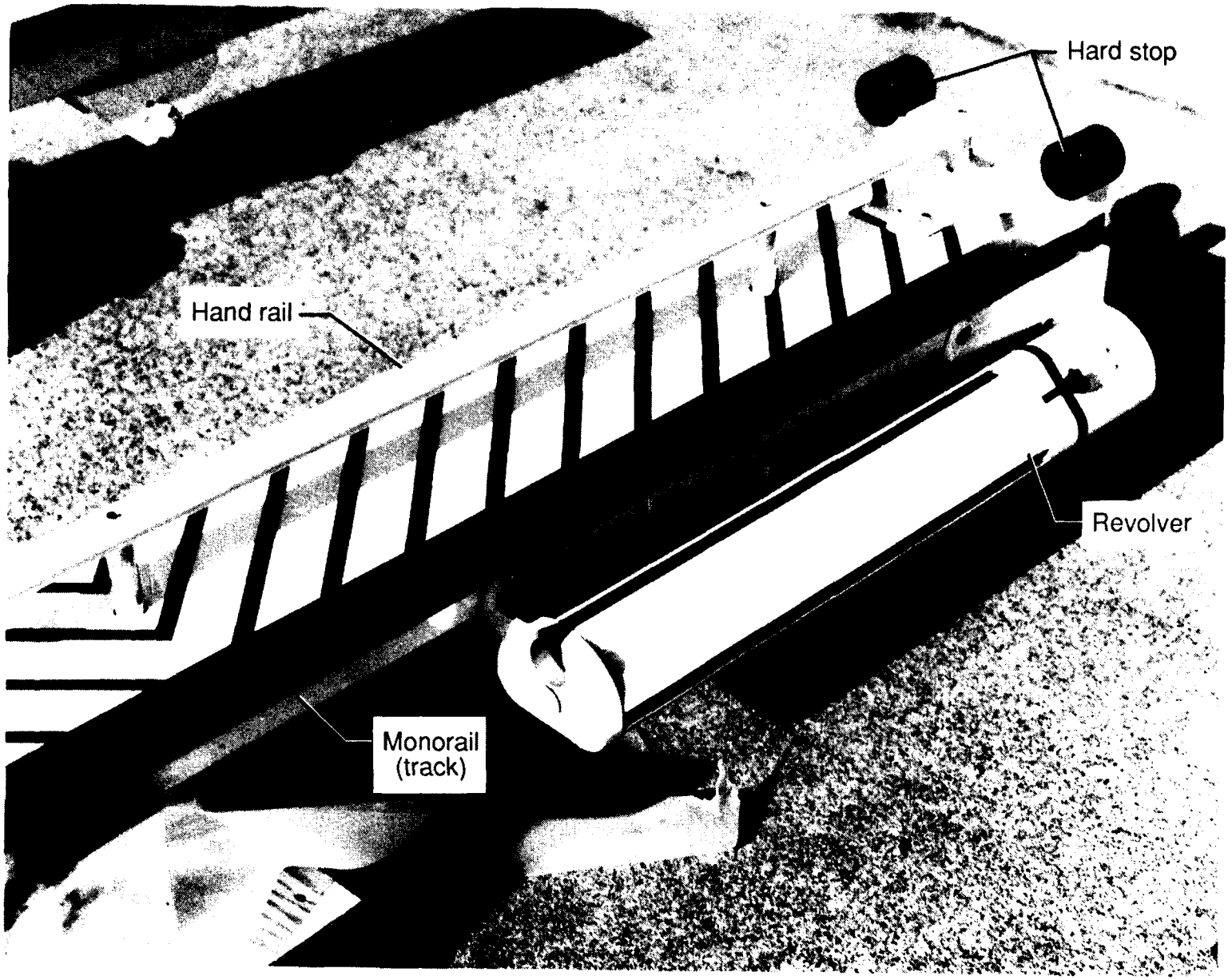

(a) Flight hardware revolver. L-91-12

Figure 2. Revolver mechanisms at end of CETA track.

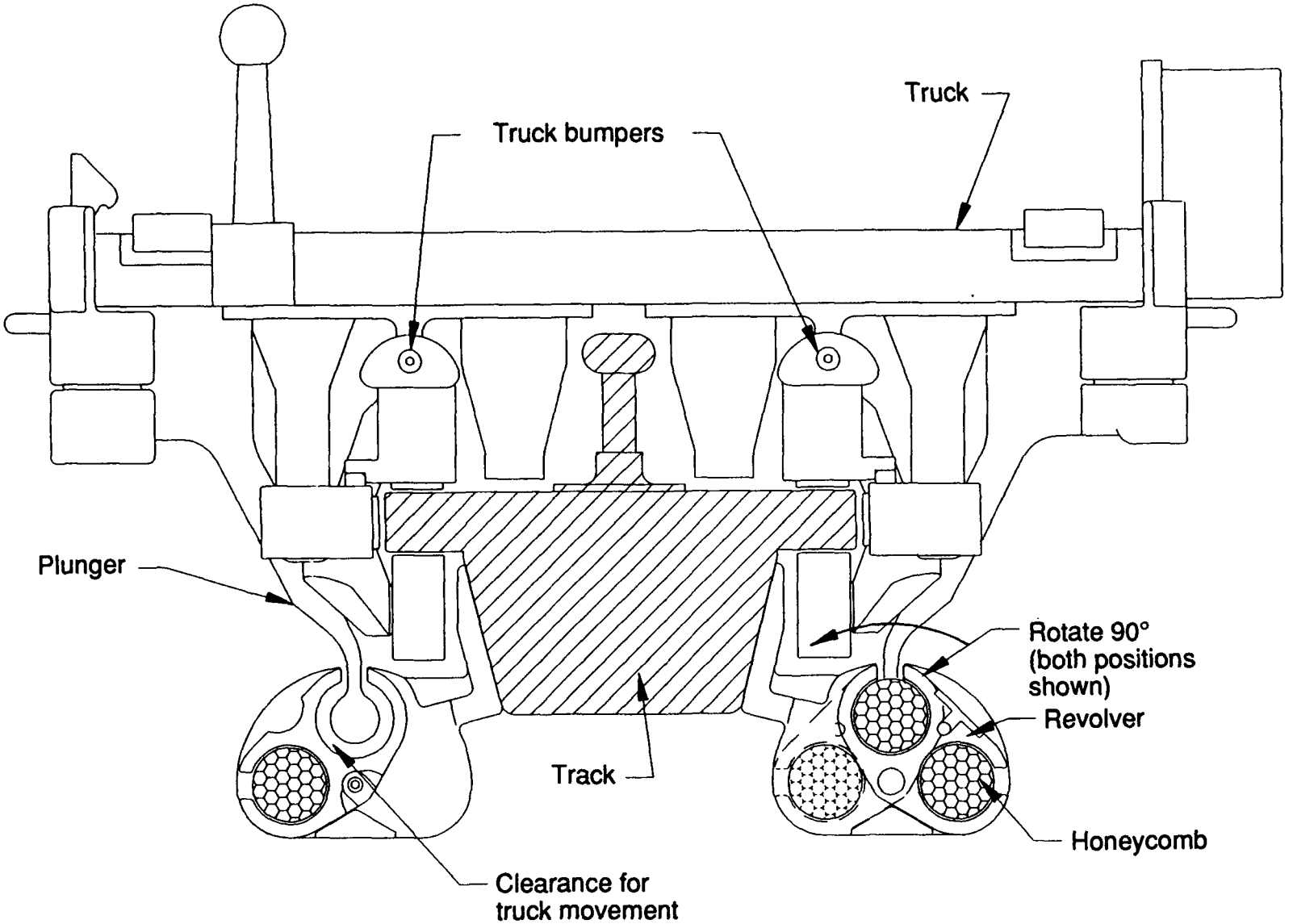

(b) Schematic end view of CETA track and revolvers on each side of track.

Figure 2. Continued.

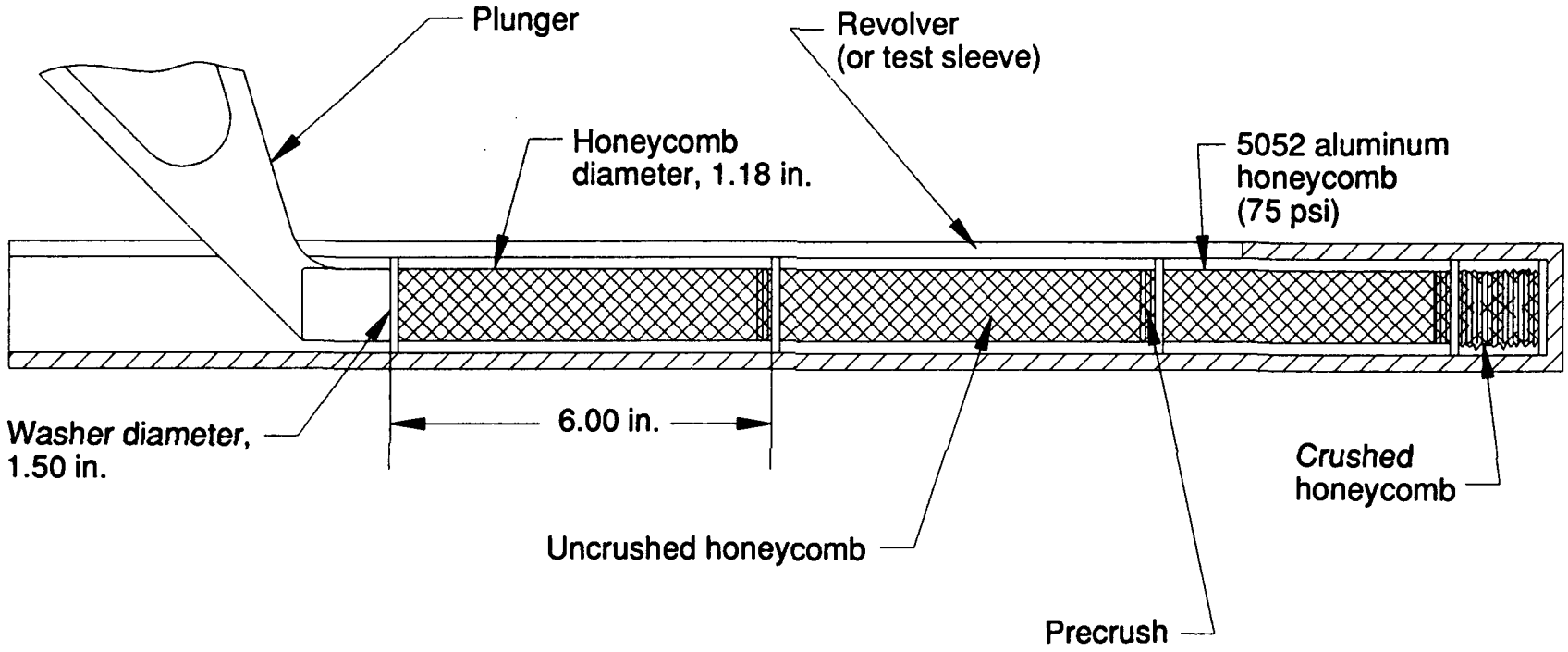

(c) Schematic drawing of honeycomb energy-absorbing tube inside revolver.

Figure 2. Concluded.

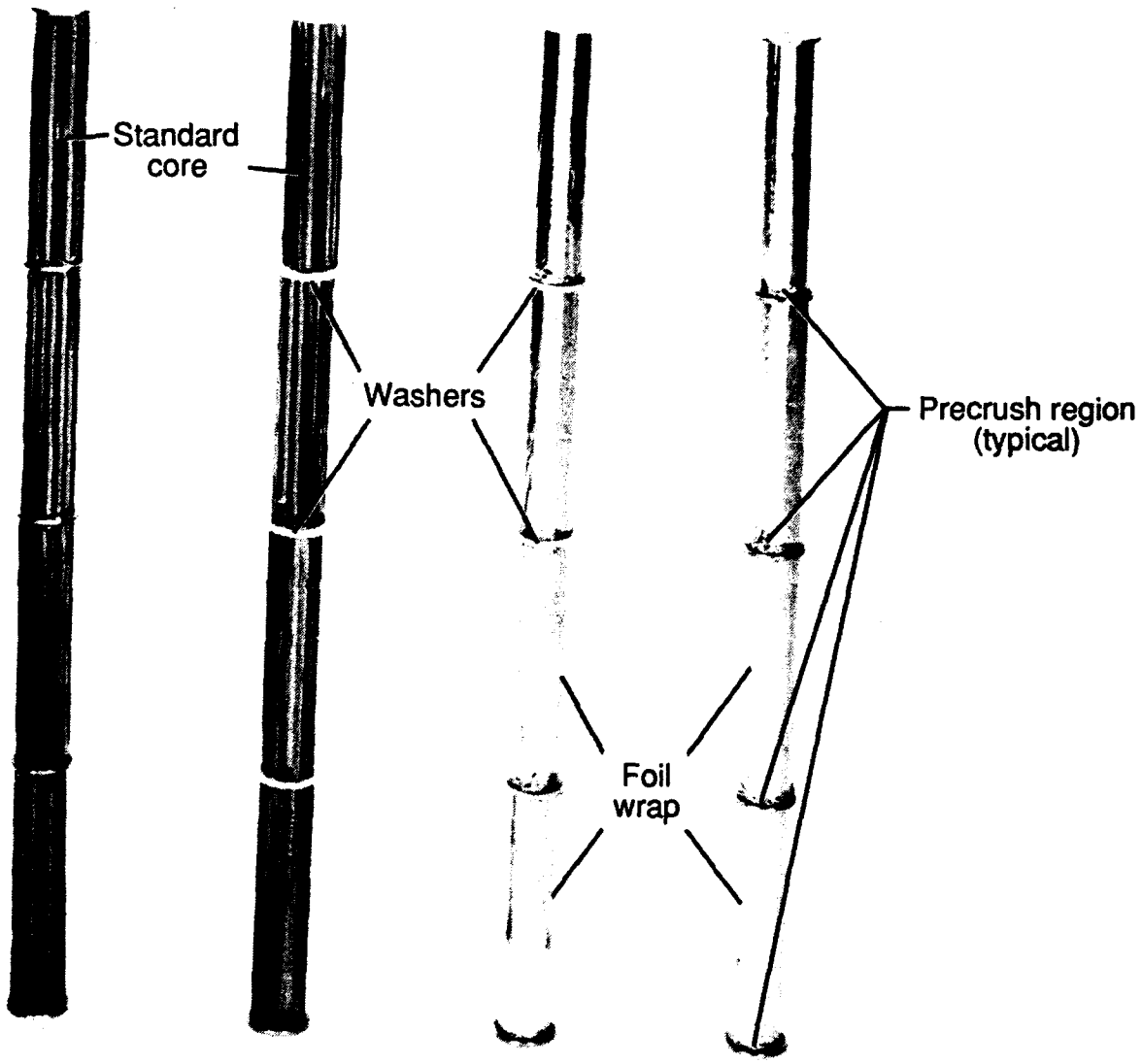

L-91-13

(a) Four honeycomb energy-absorbing specimens.

Figure 3. Details of honeycomb test specimens.

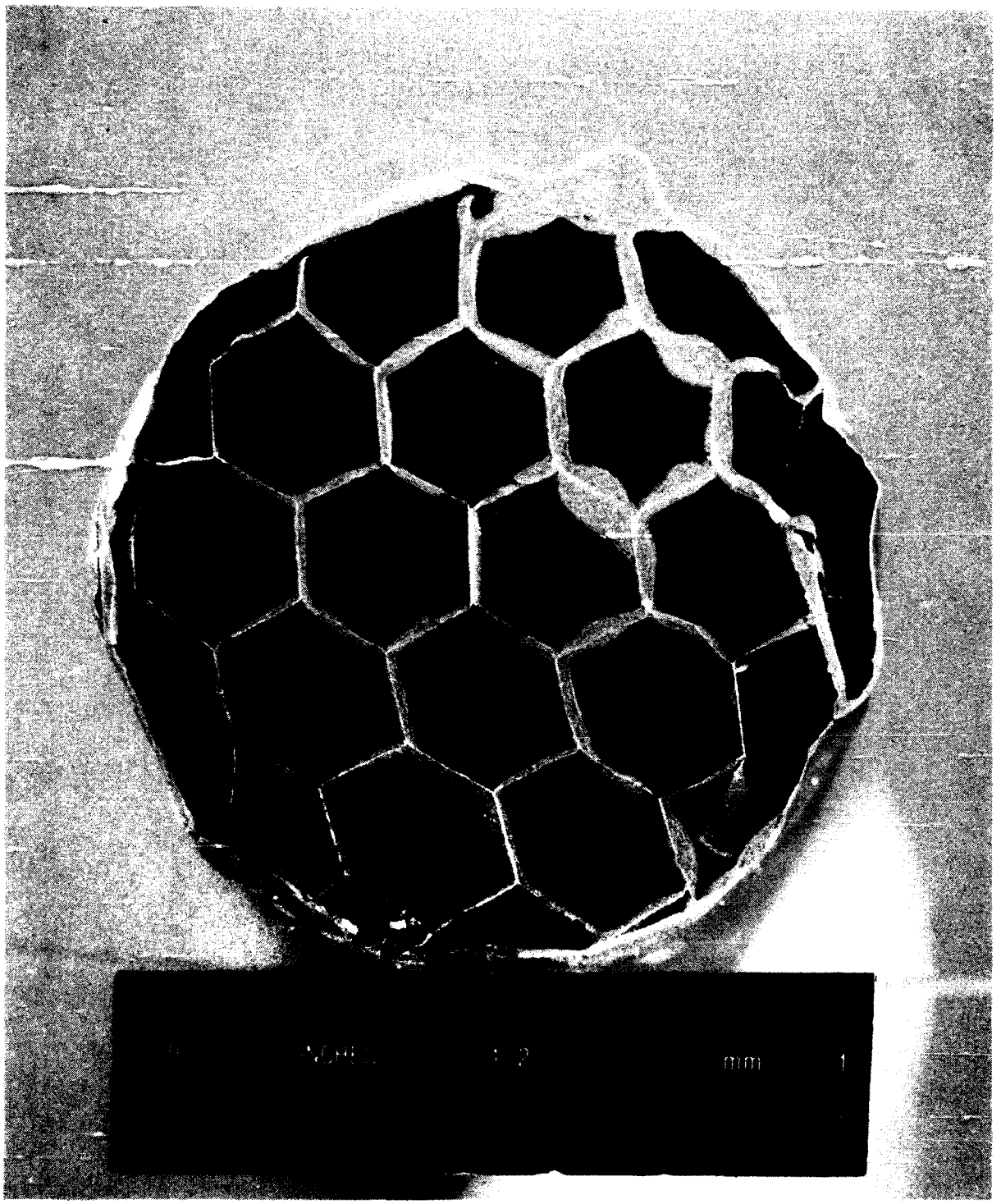

L-90-6375

(b) Honeycomb tube cross section.

Figure 3. Concluded.

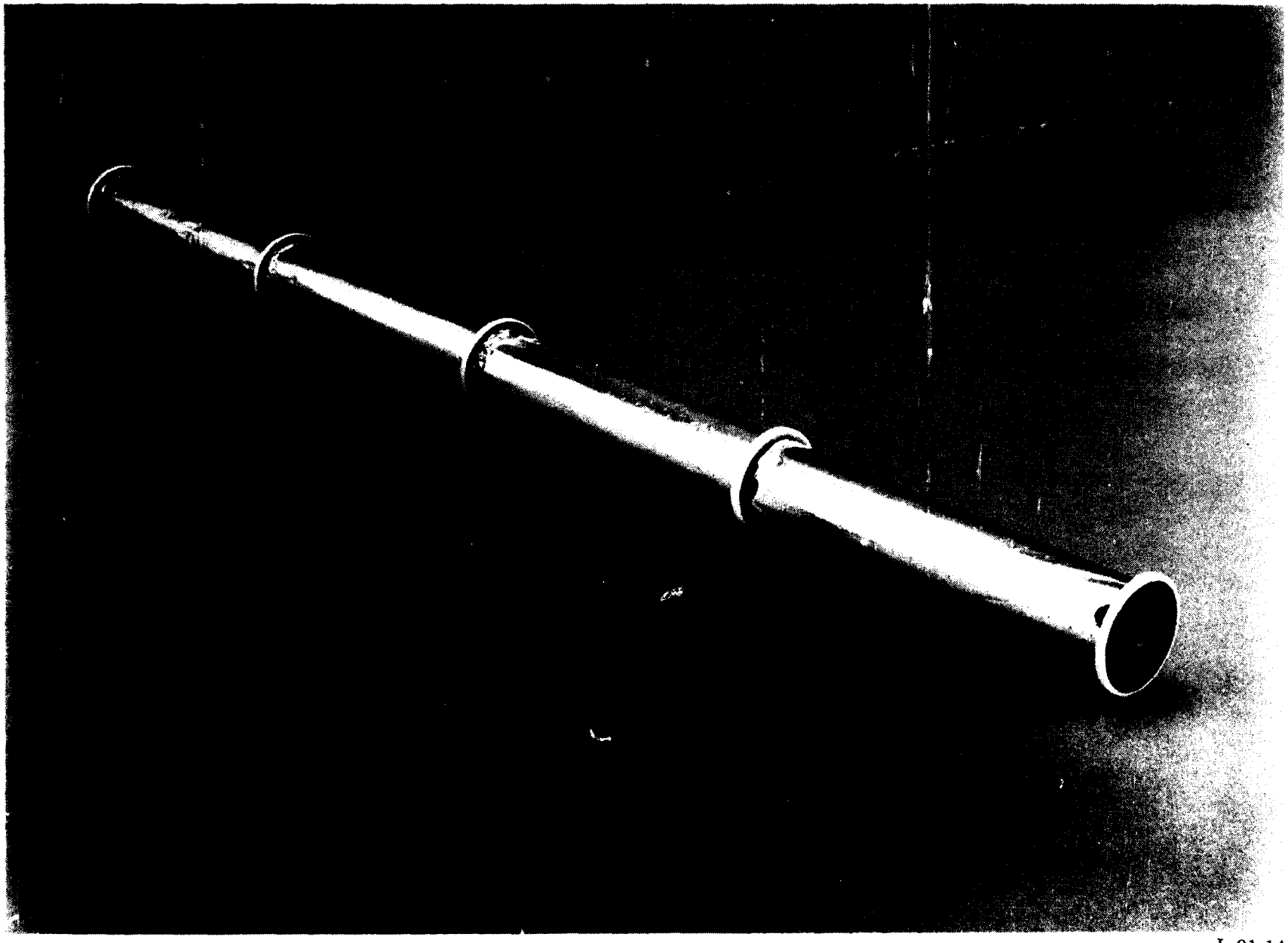

L-91-14

Figure 4. Standard core honeycomb with foil wrap energy absorber.

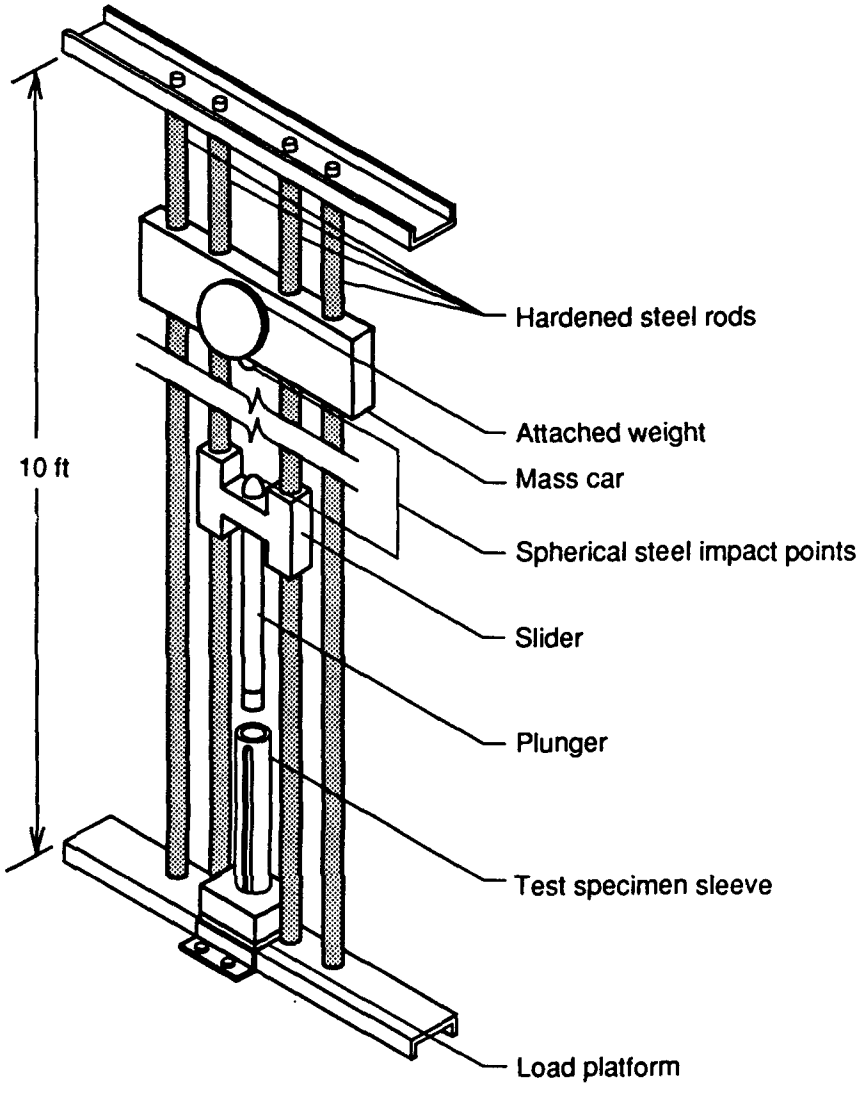

Figure 5. Drop tower used for impact testing of honeycomb energy absorbers.

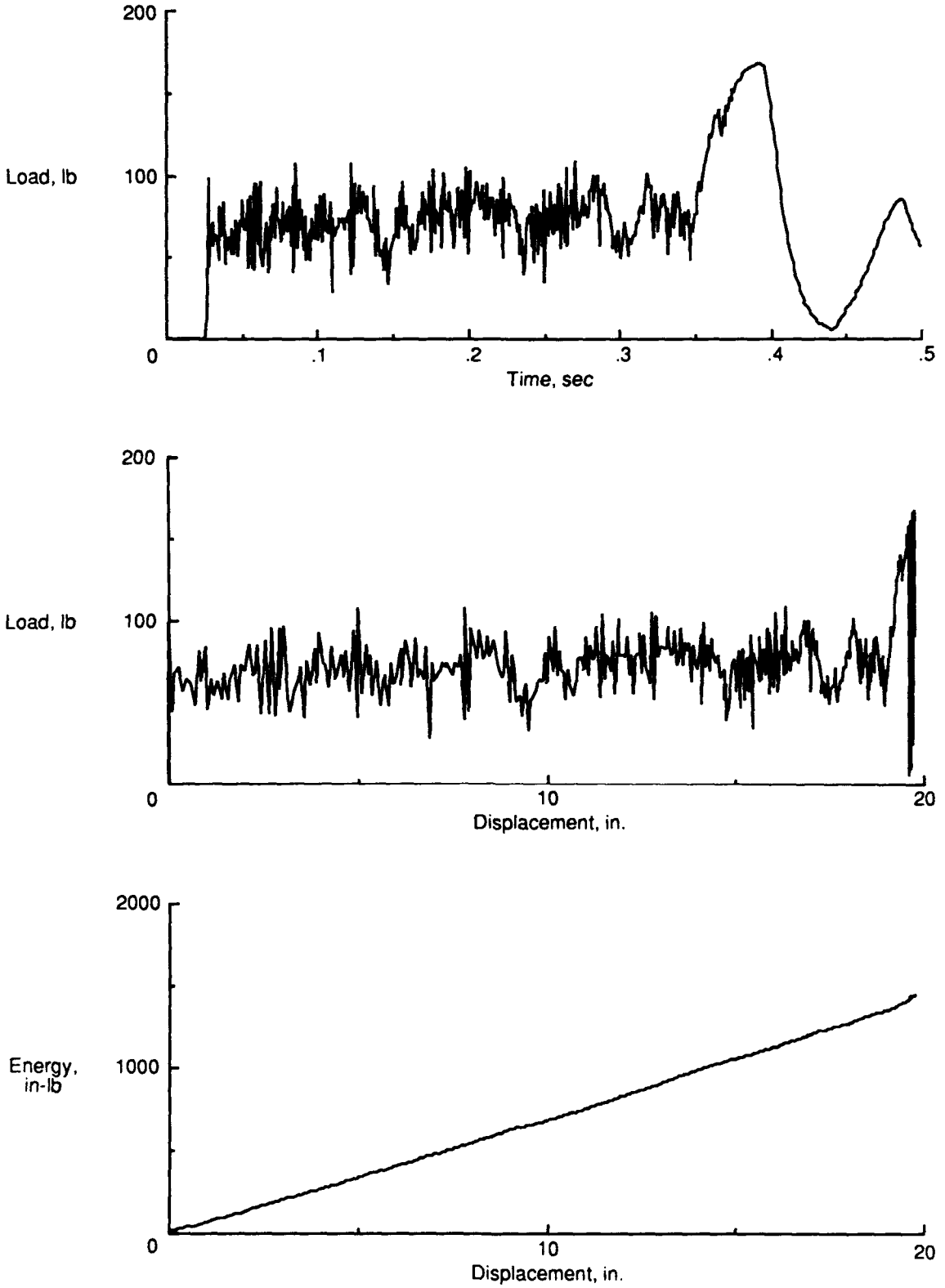

Figure 6. Test 1 specimen type TCA.

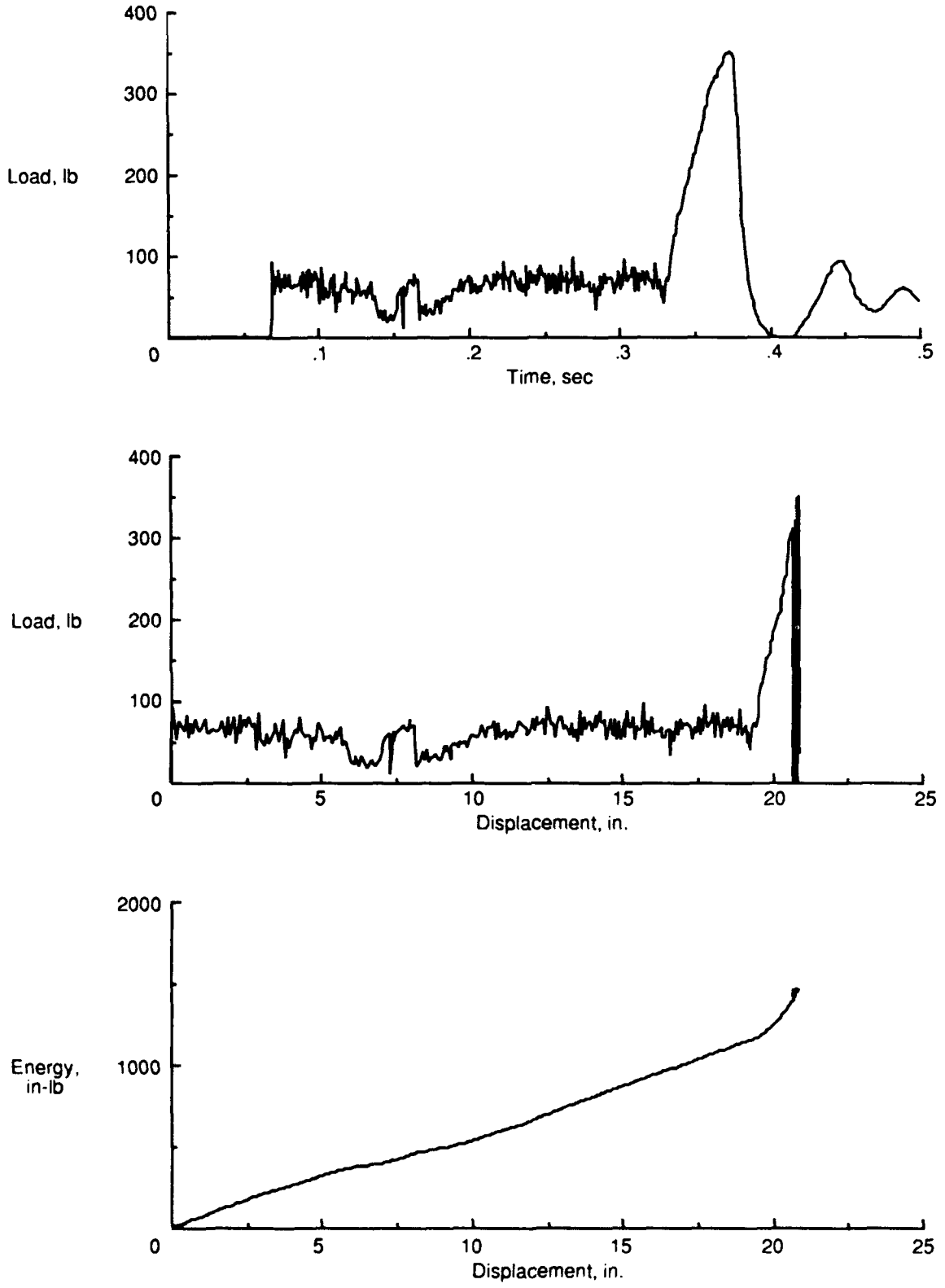

Figure 7. Test 2 specimen type TCP.

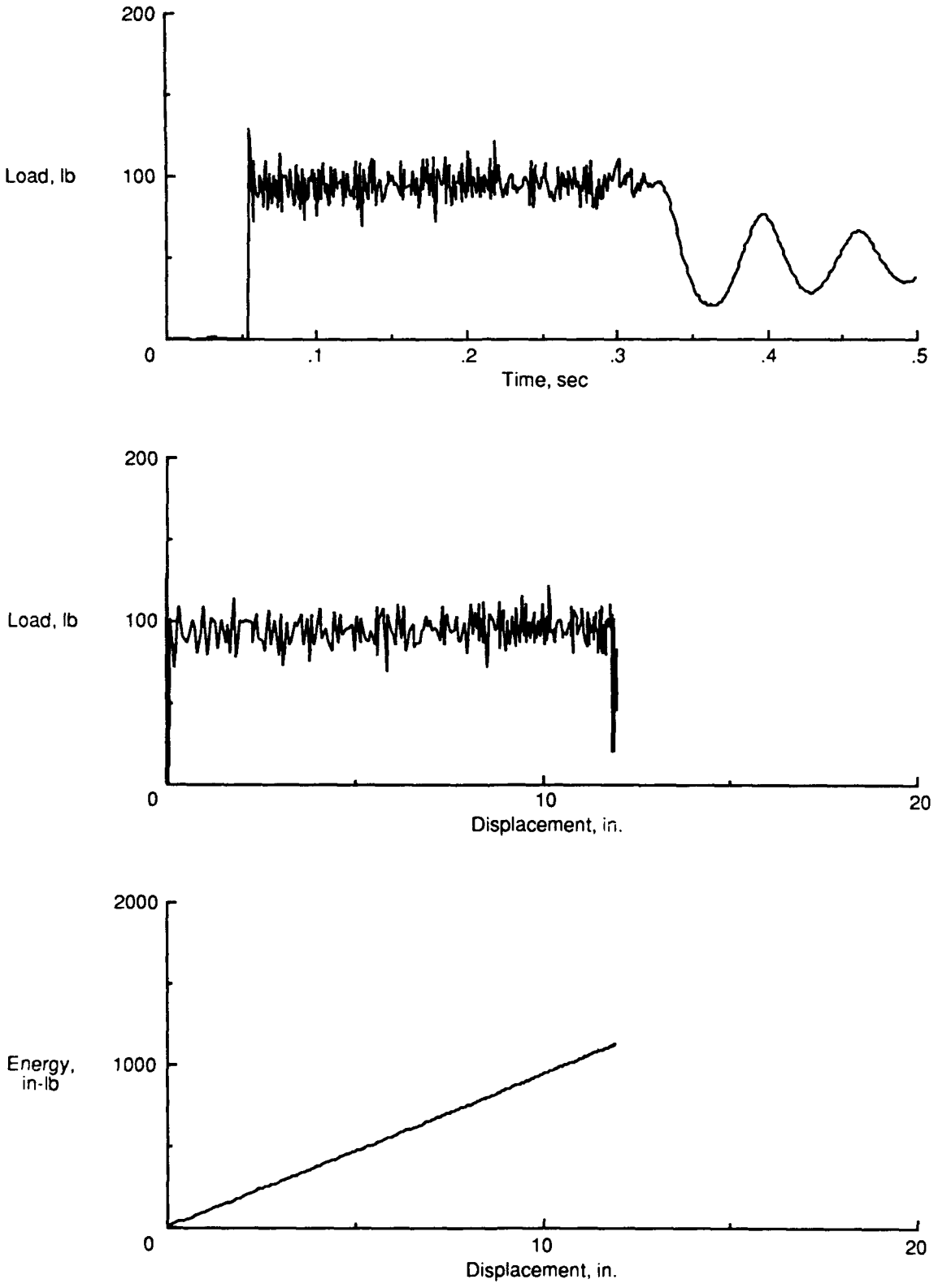

Figure 8. Test 3 specimen type SCP.

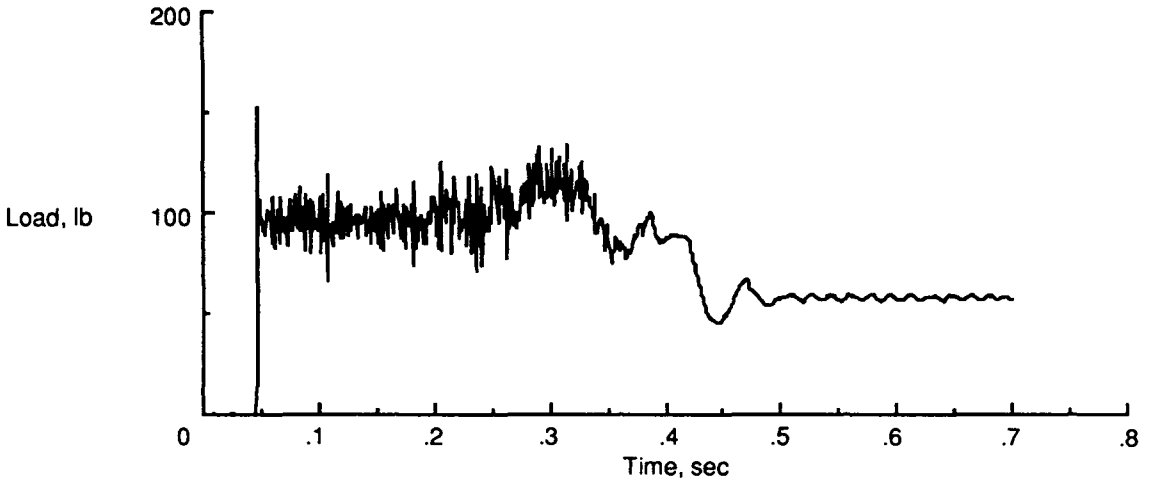

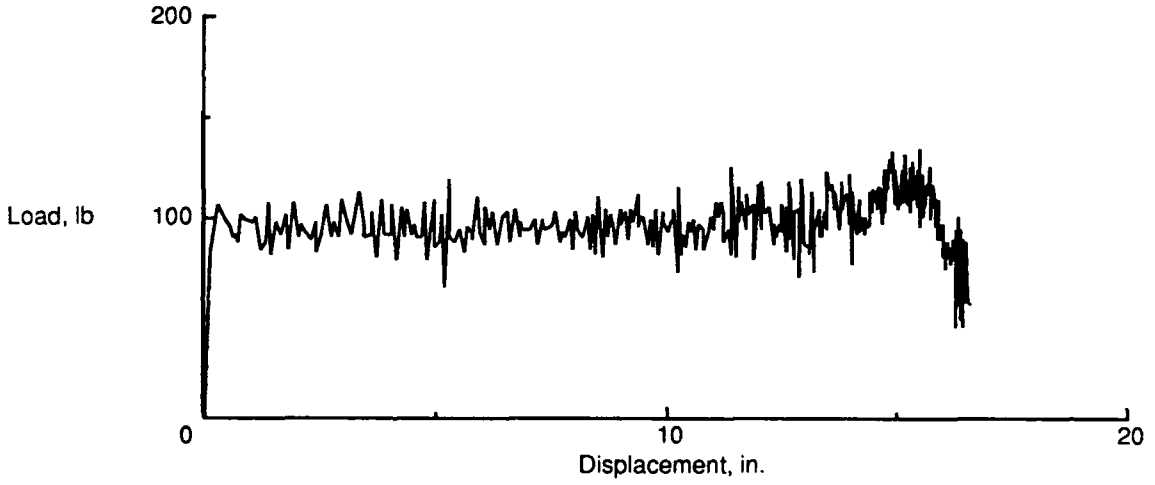

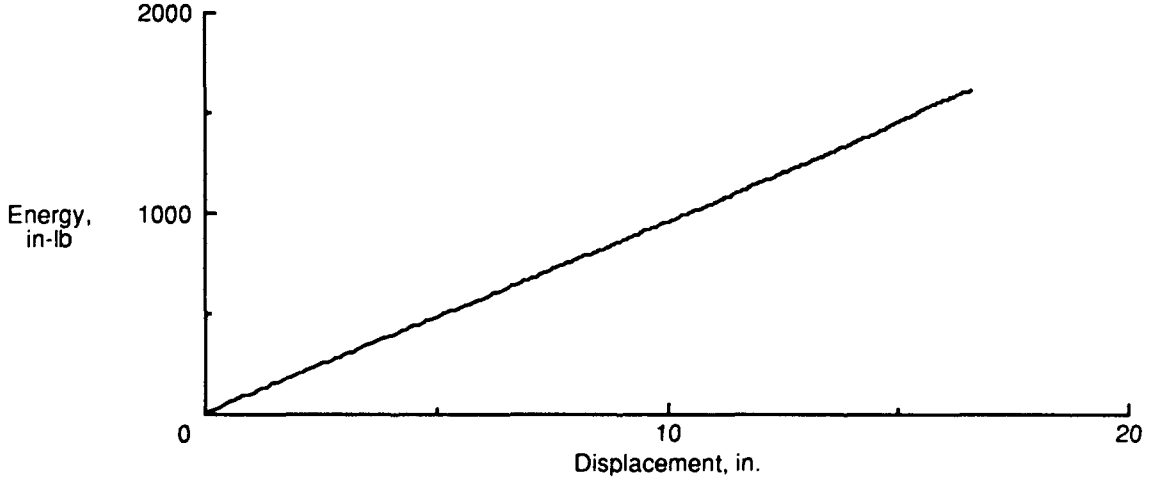

Figure 9. Test 4 specimen type SCA.

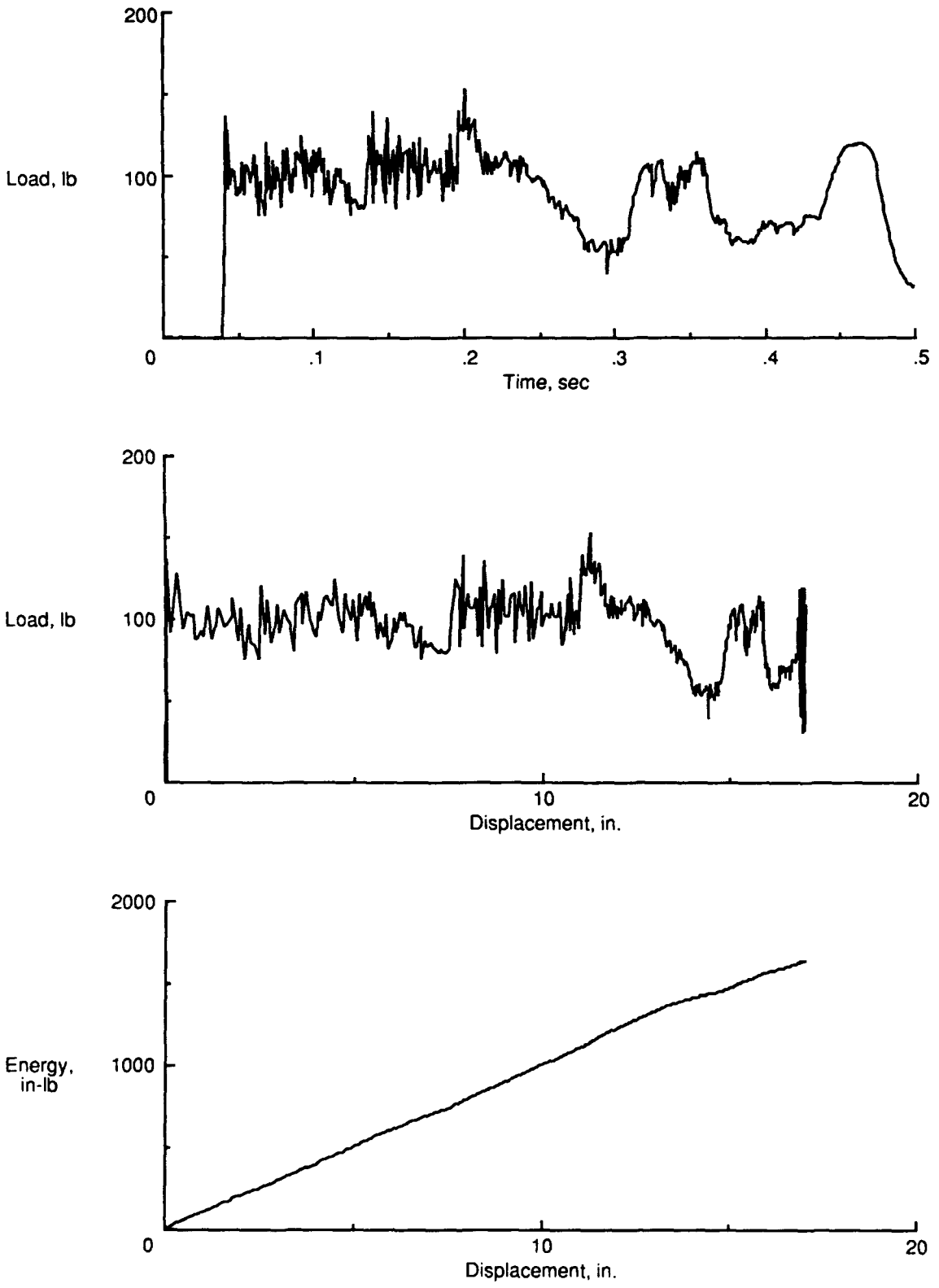

Figure 10. Test 5 specimen type SCPF.

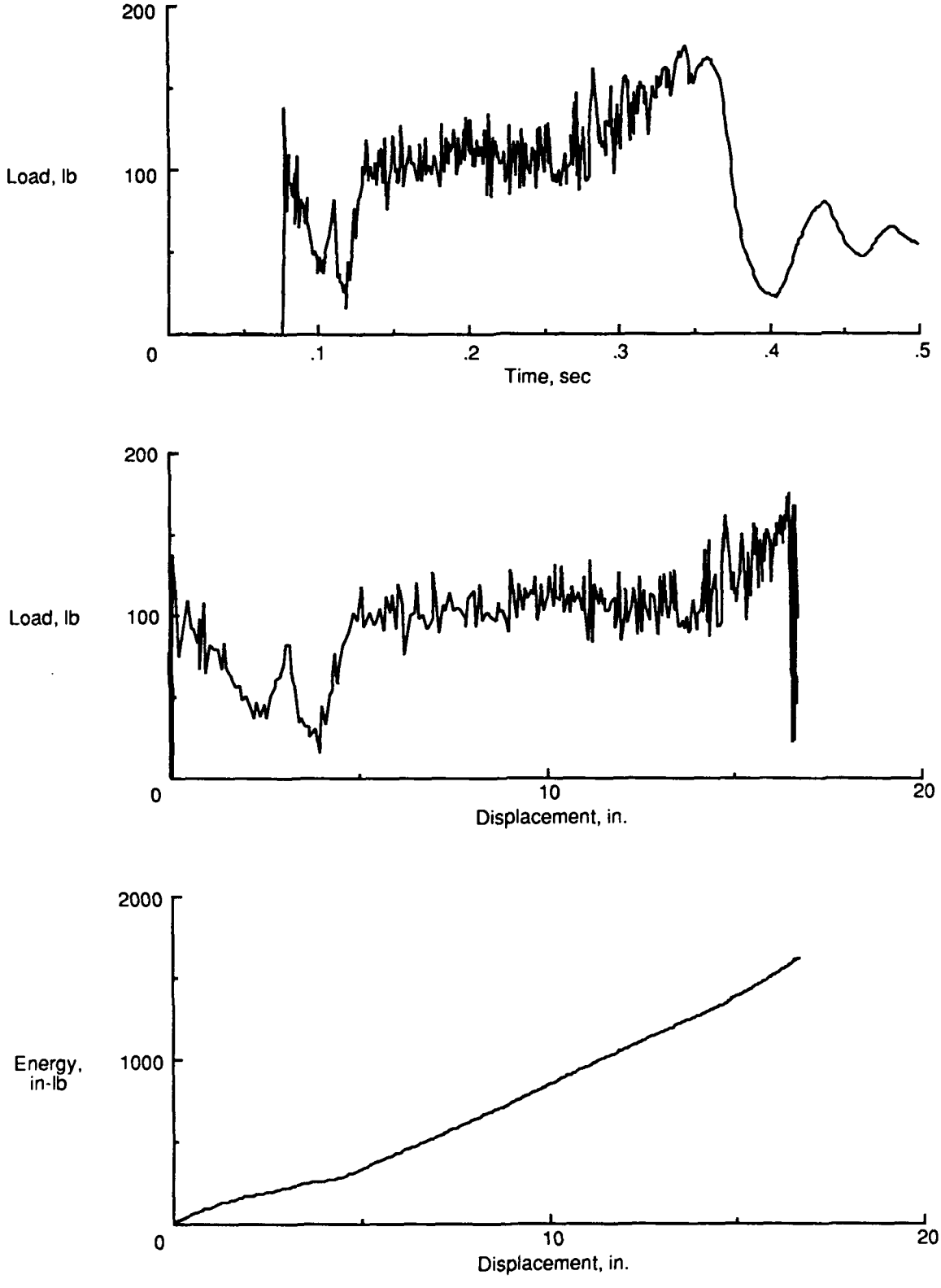

Figure 11. Test 6 specimen type SCAF.

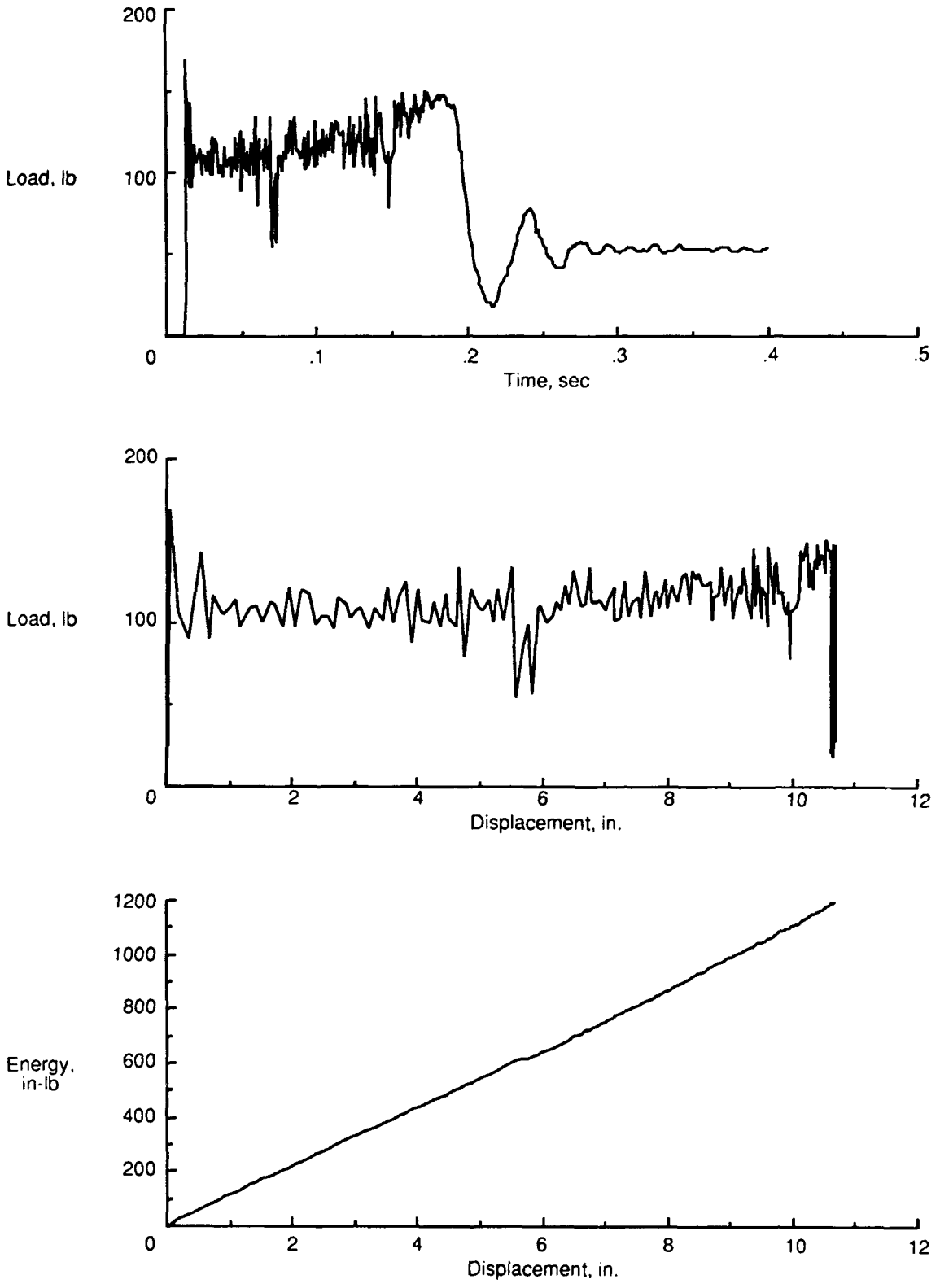

Figure 12. Test 7 specimen type SCAF.

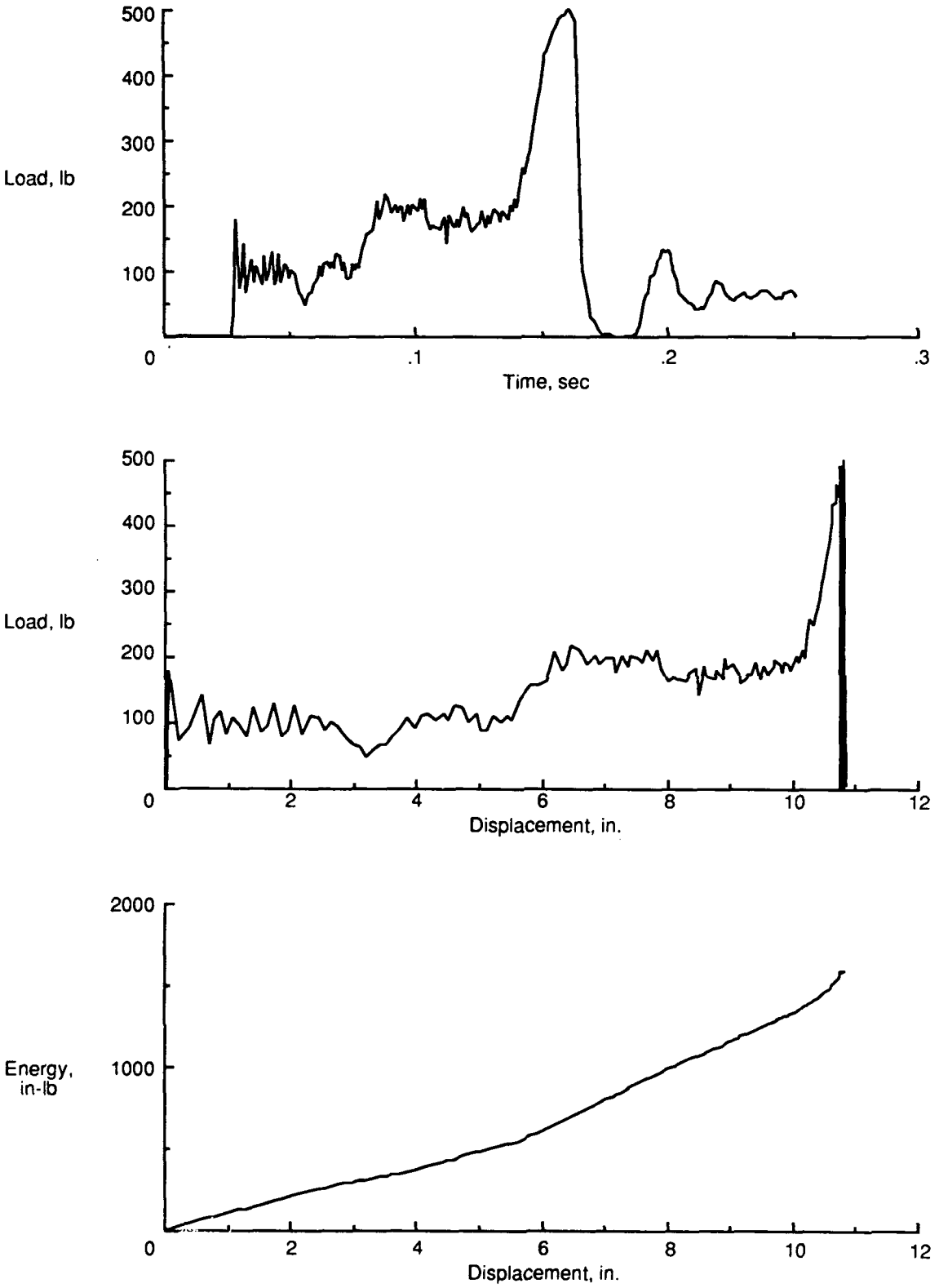

Figure 13. Test 8 specimen type SCAF.

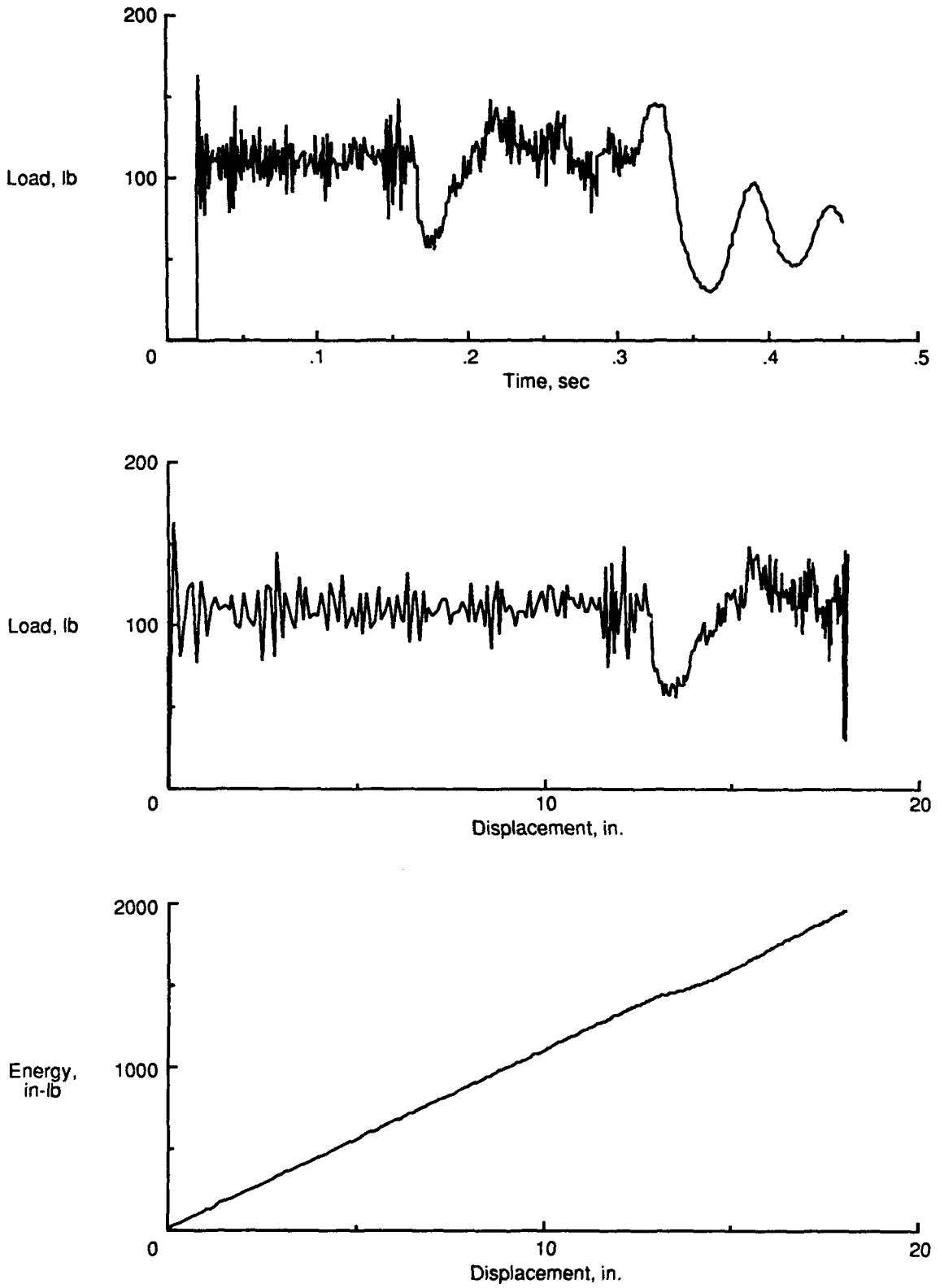

Figure 14. Test 9 specimen type SCAF.

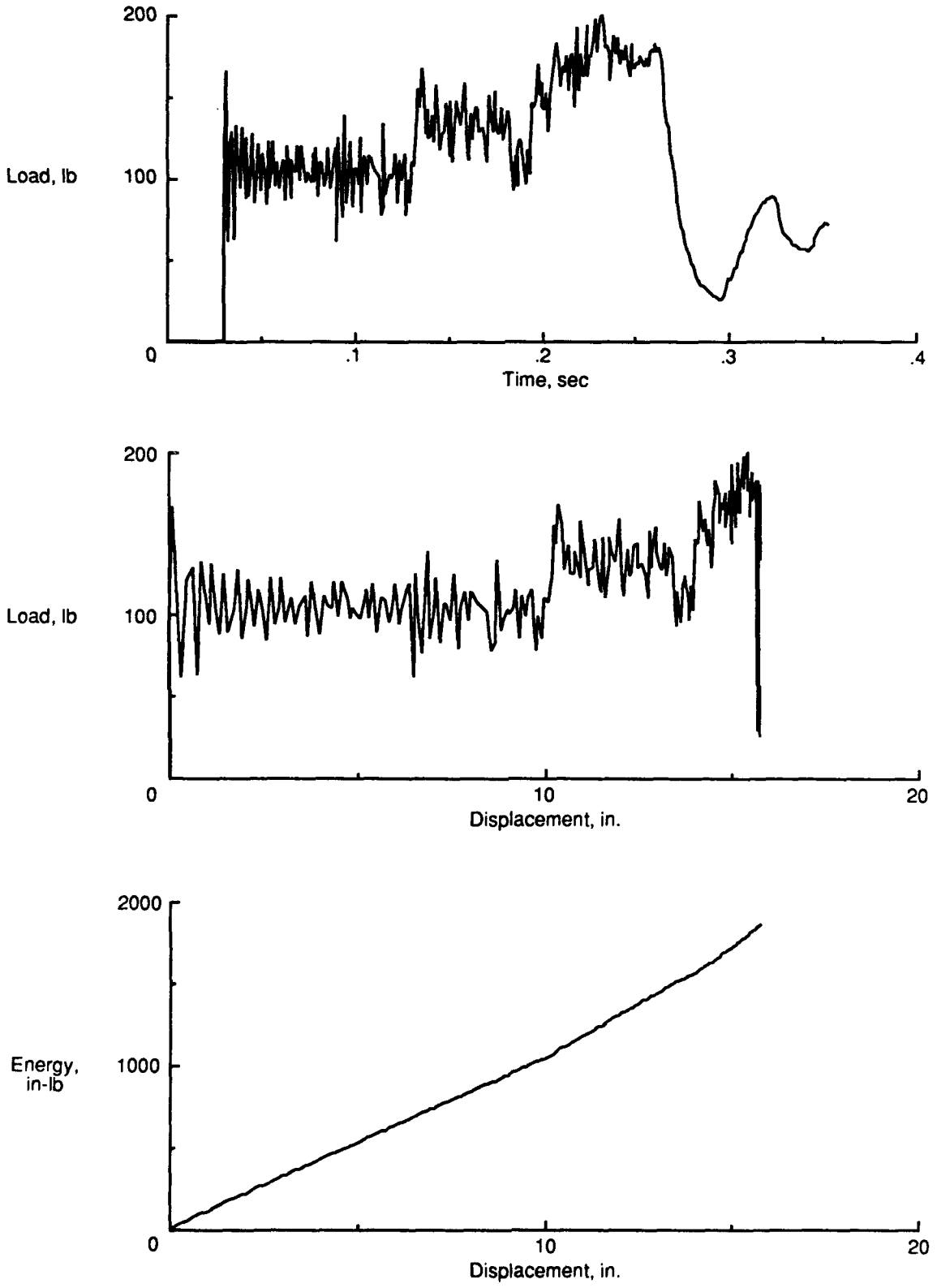

Figure 15. Test 10 specimen type SCAF.

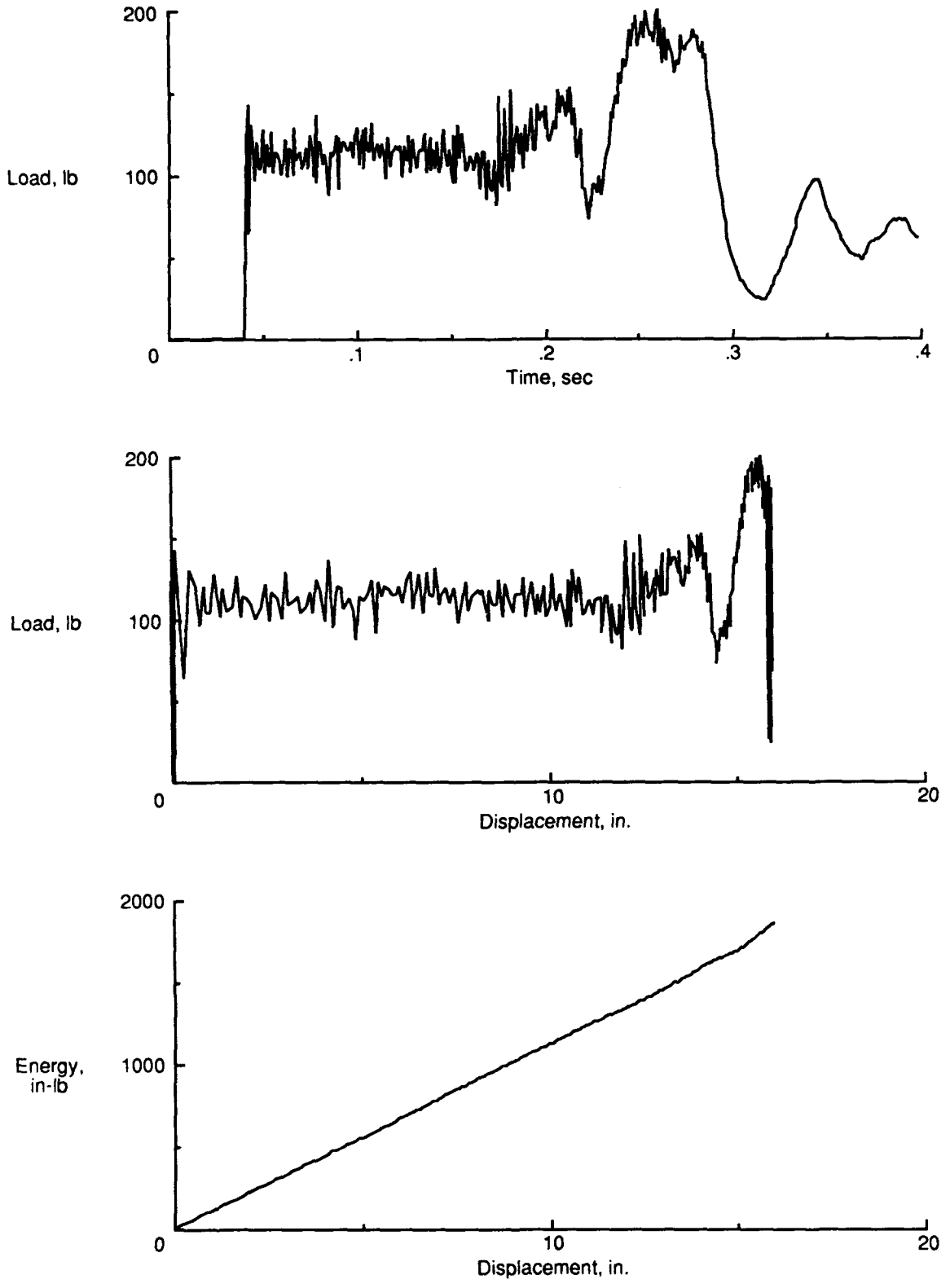

Figure 16. Test 11 specimen type SCAF.

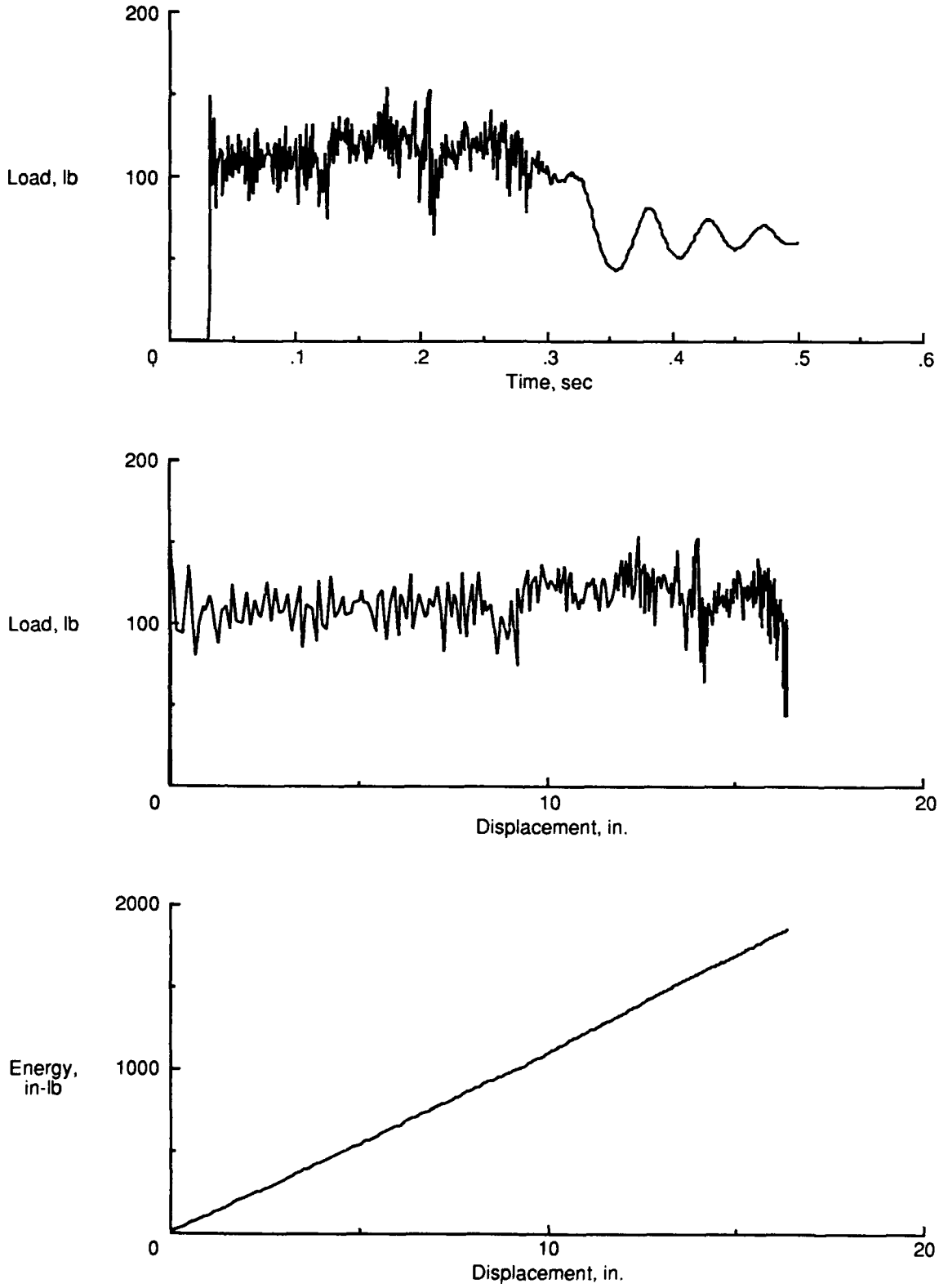

Figure 17. Test 12 specimen type SCAF.

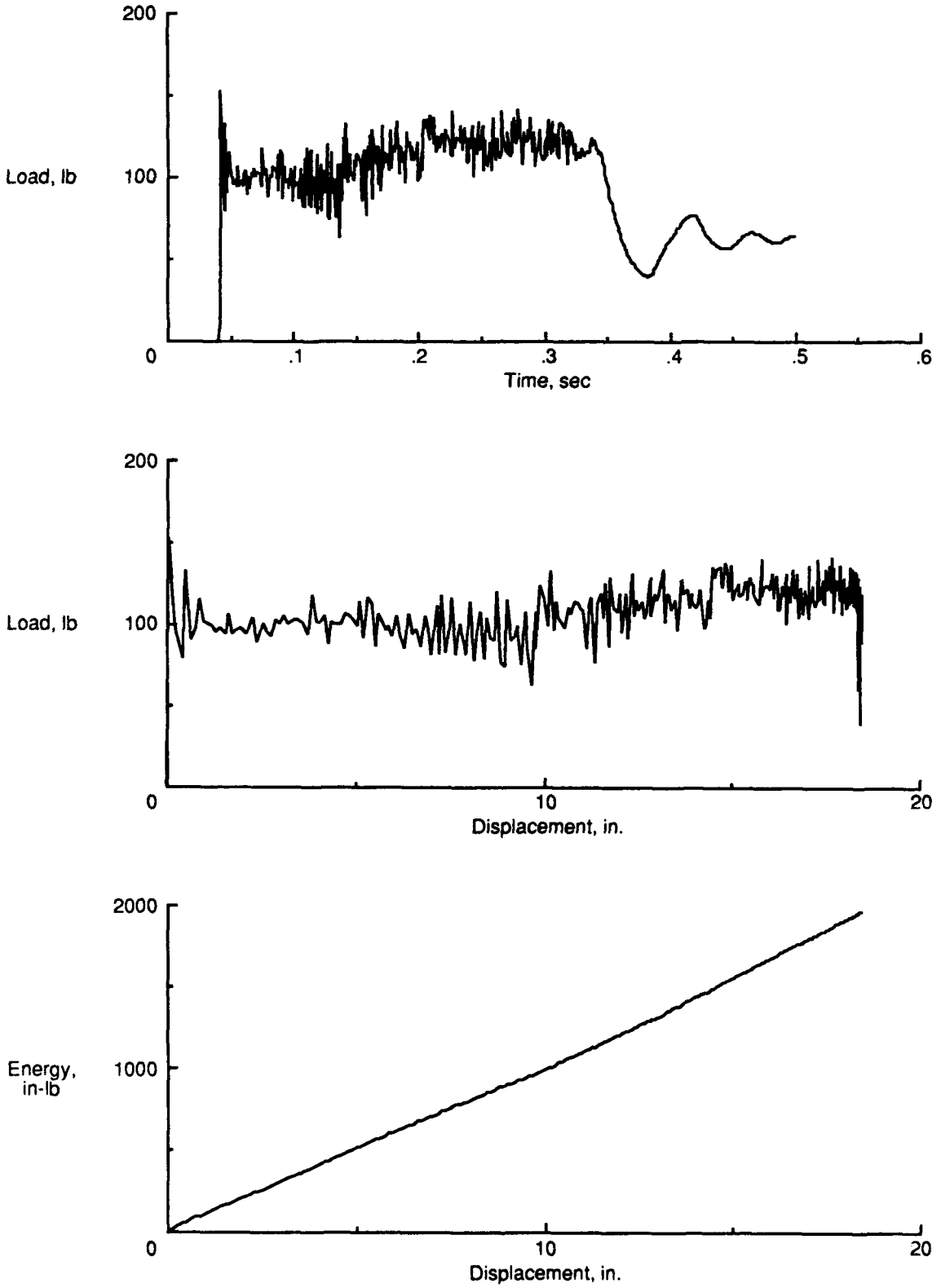

Figure 18. Test 13 specimen type SCTF.

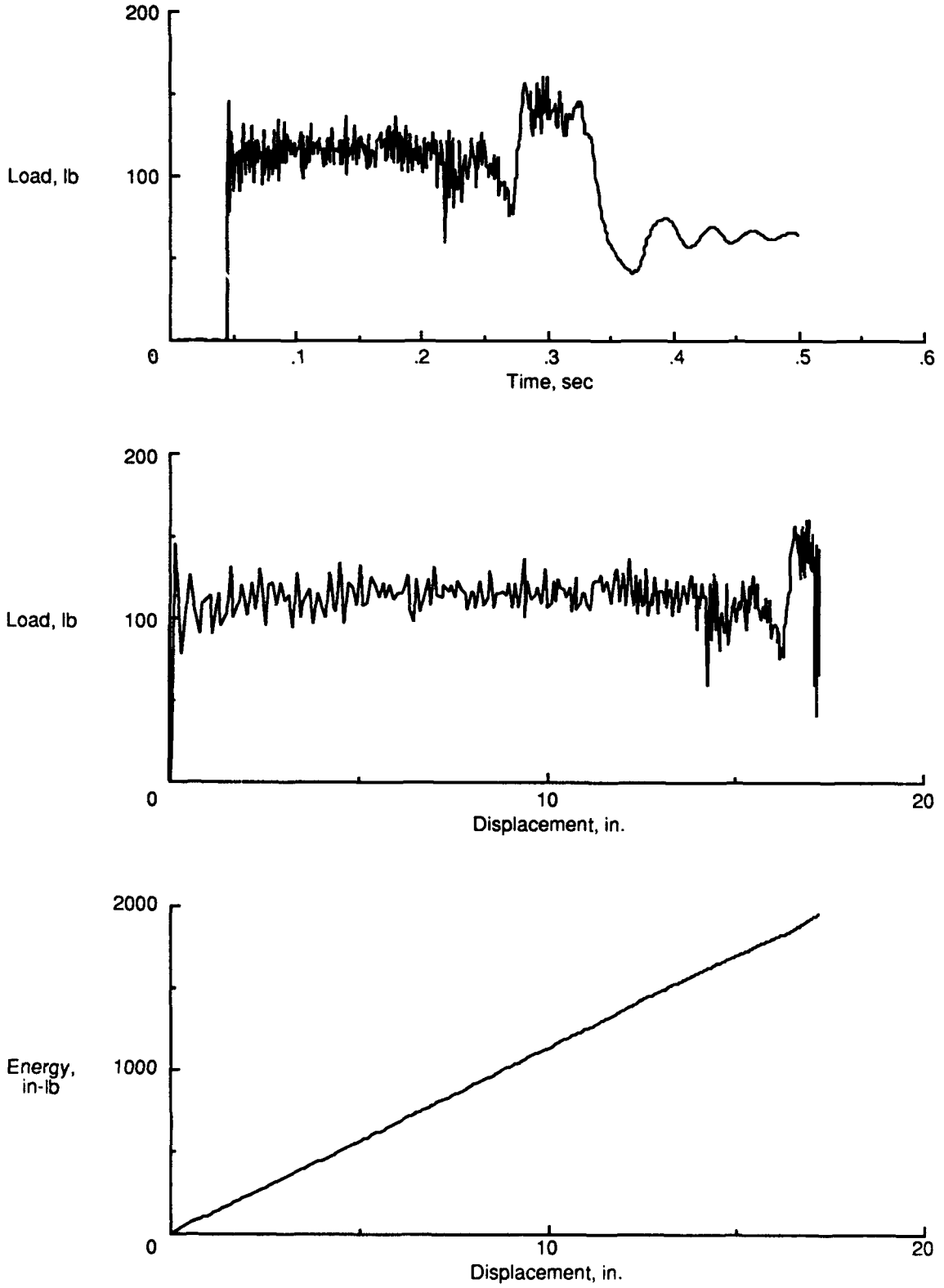

Figure 19. Test 14 specimen type SCTF.

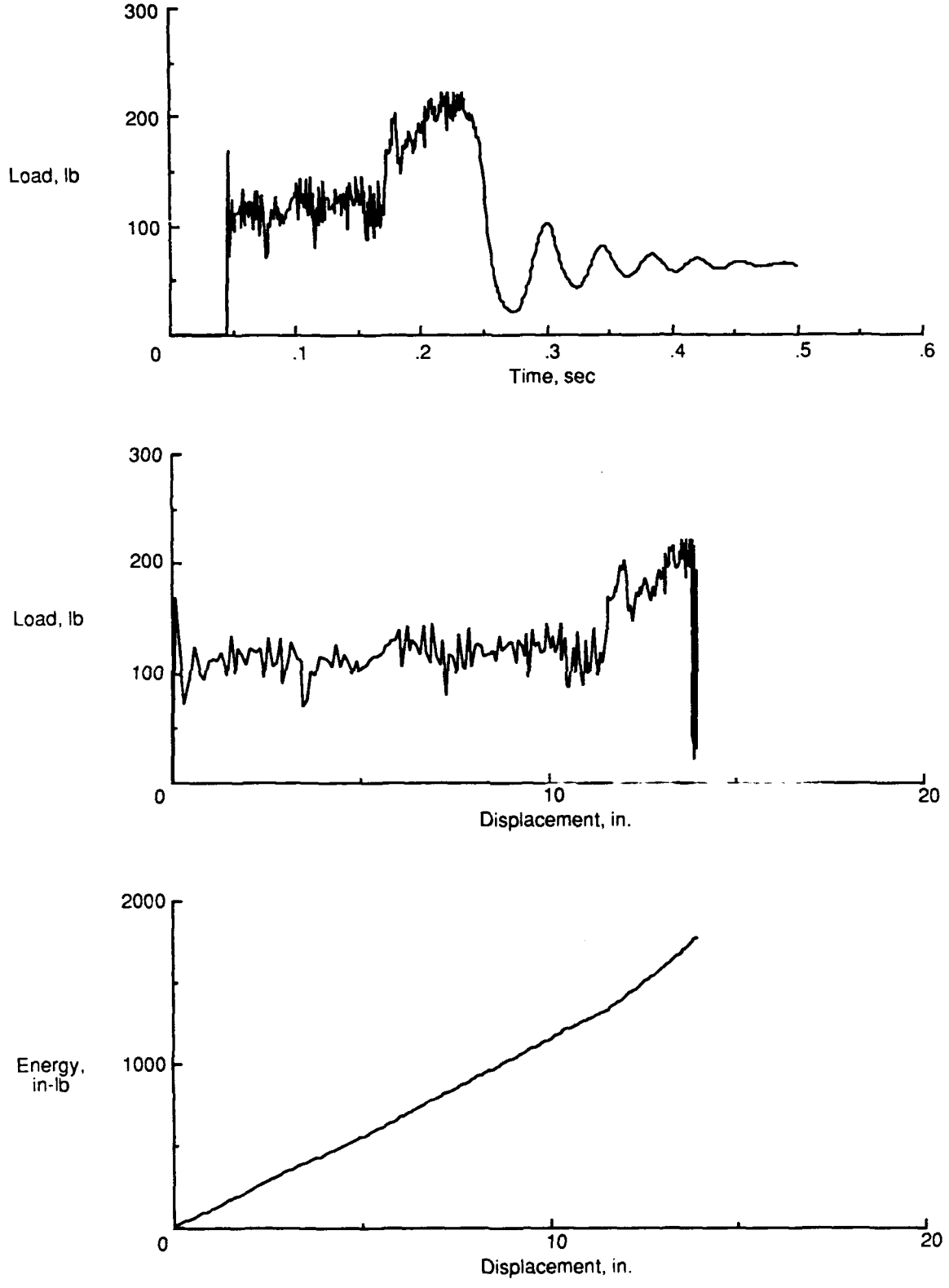

Figure 20. Test 15 specimen type SCTF.

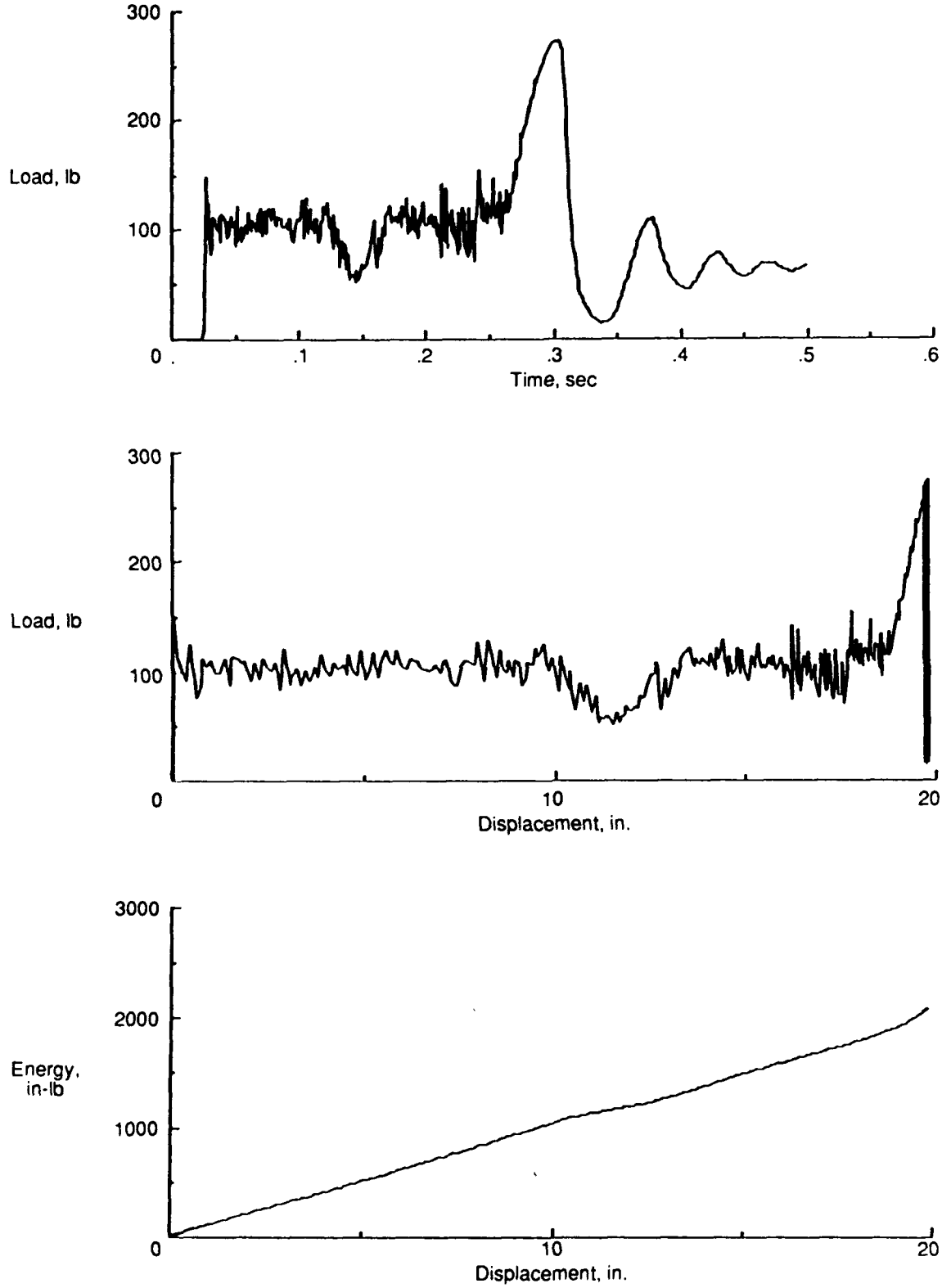

Figure 21. Test 16 specimen type SCTF.

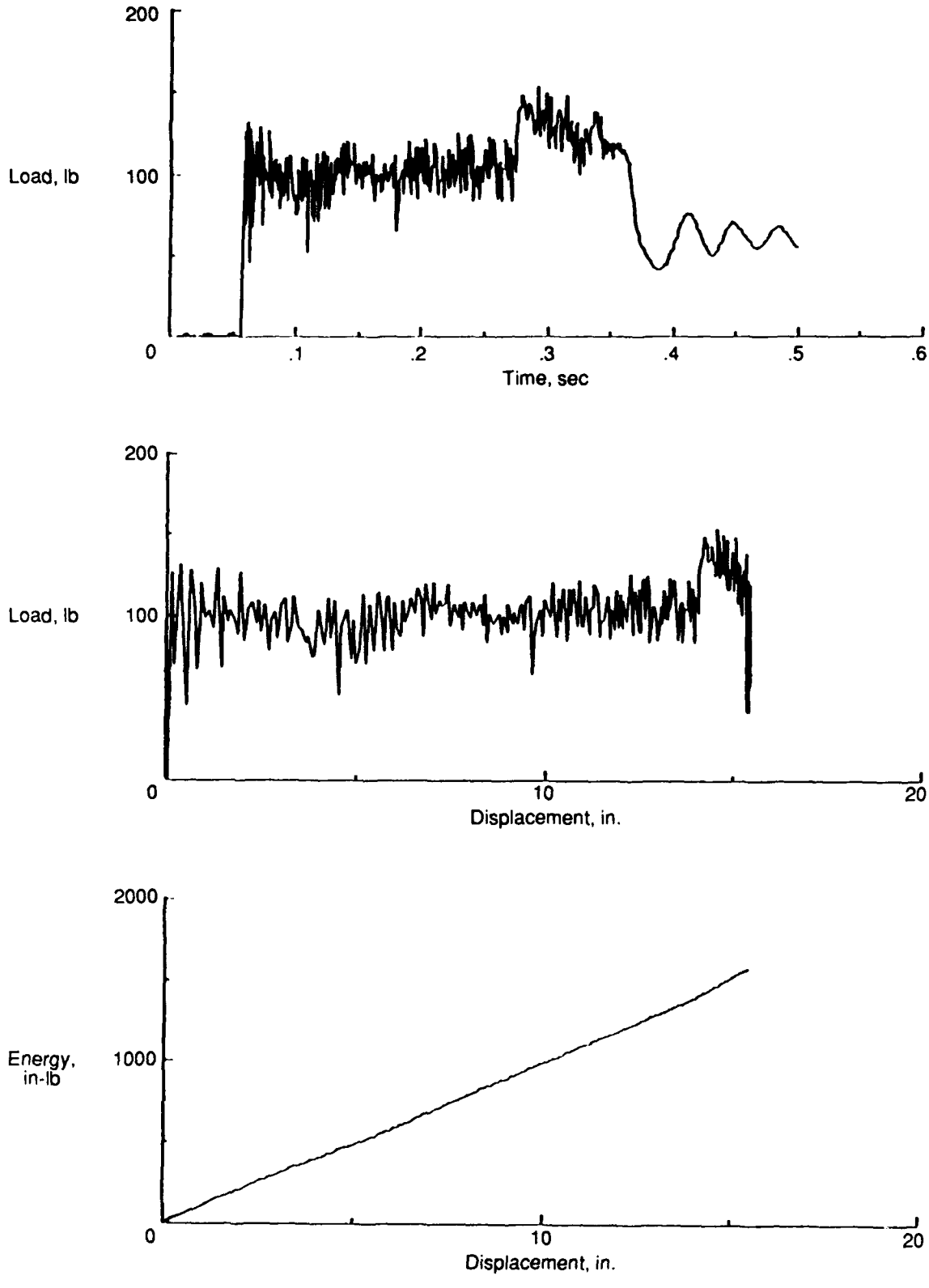

Figure 22. Test 17 specimen type SCTF (in revolver).

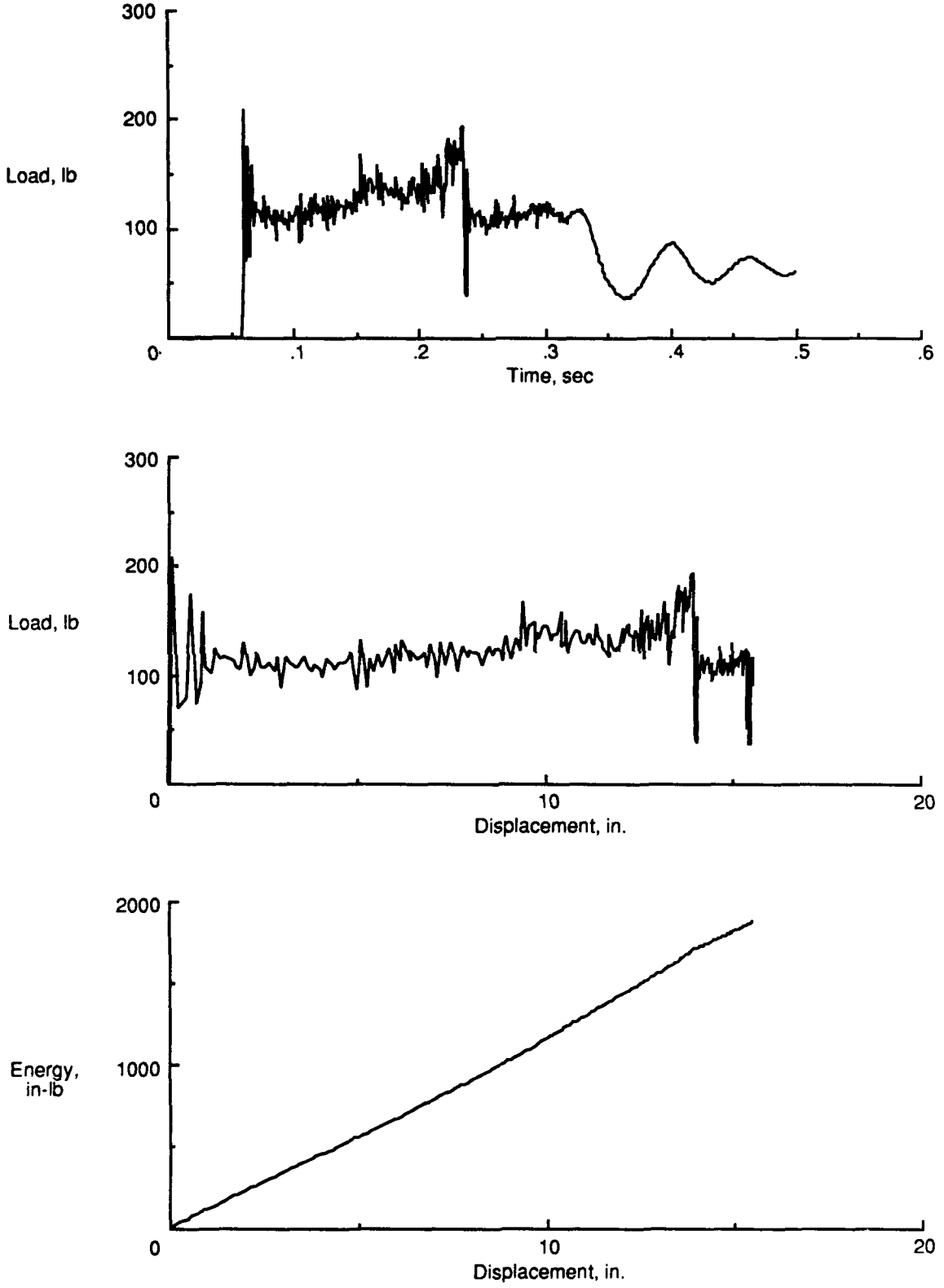

Figure 23. Test 18 specimen type SCAFM.

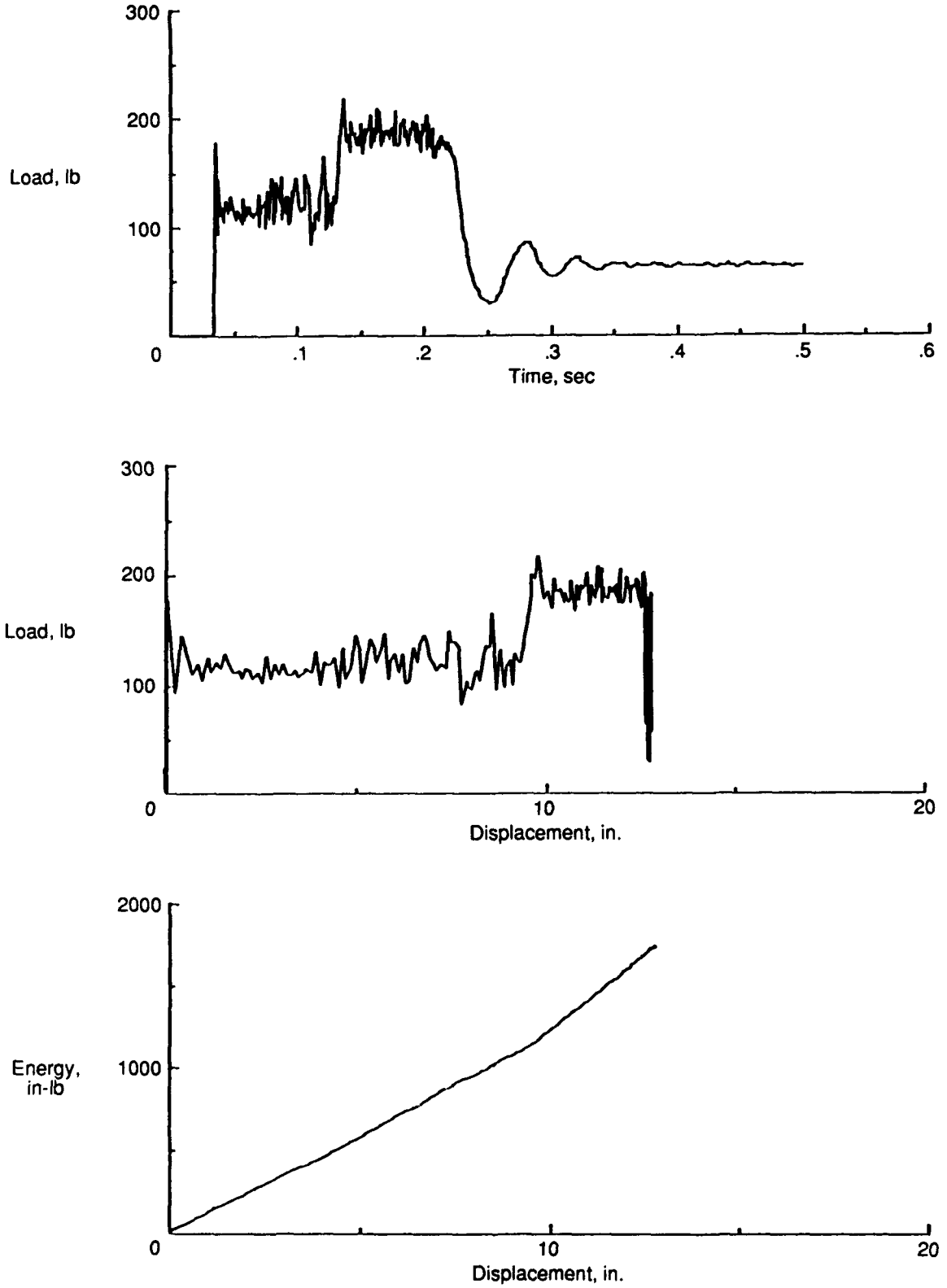

Figure 24. Test 19 specimen type SCAFM.

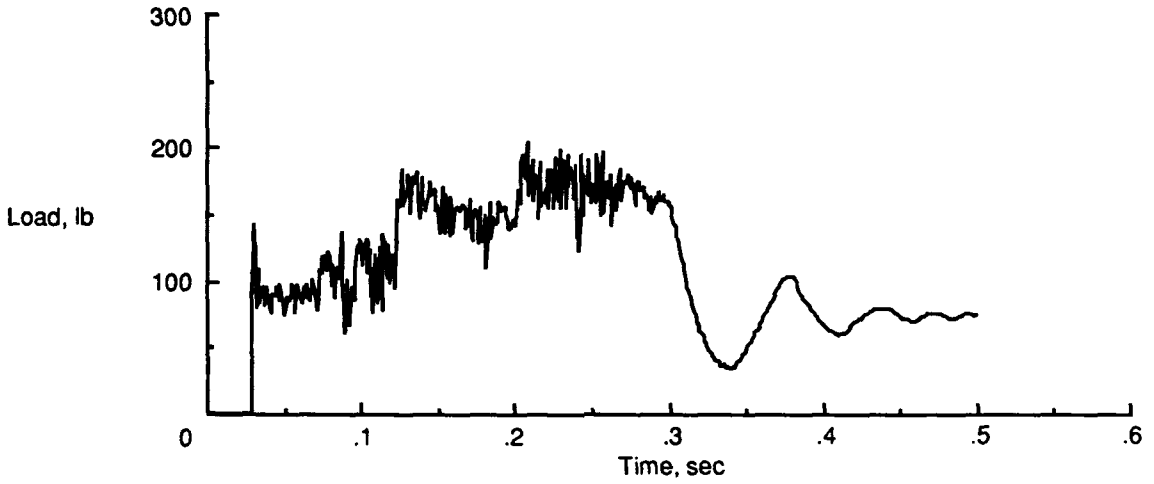

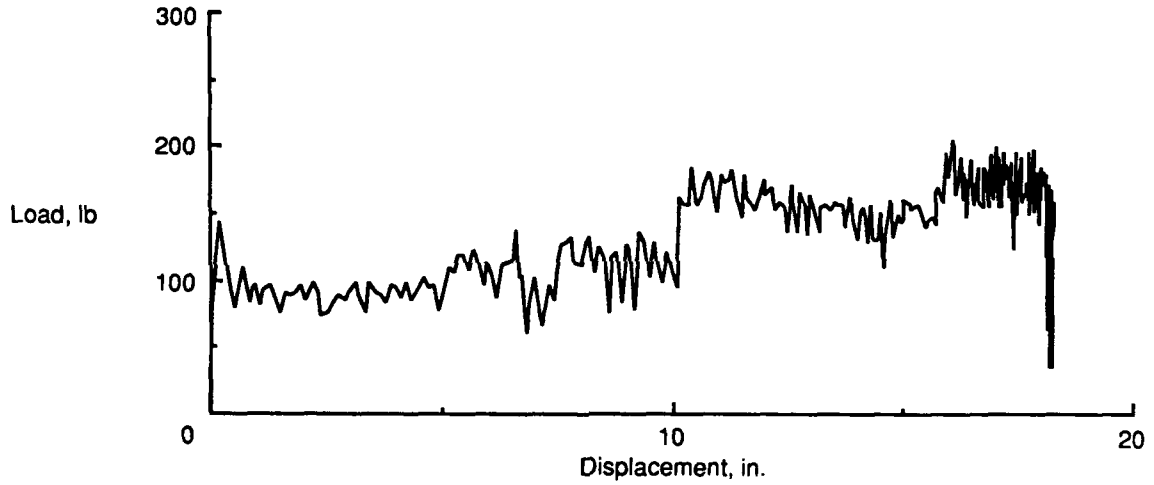

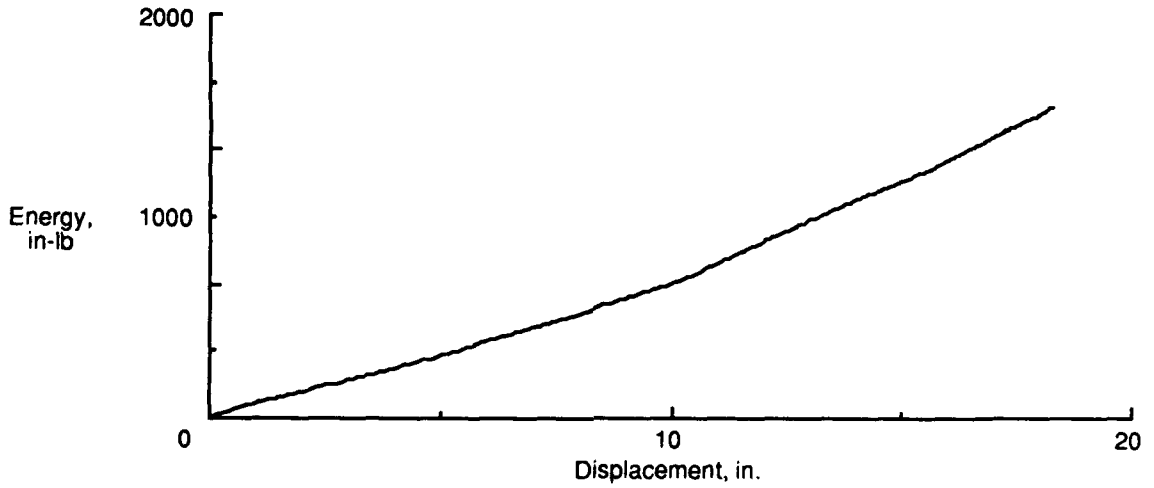

Figure 25. Test 20 specimen type SCTFS.

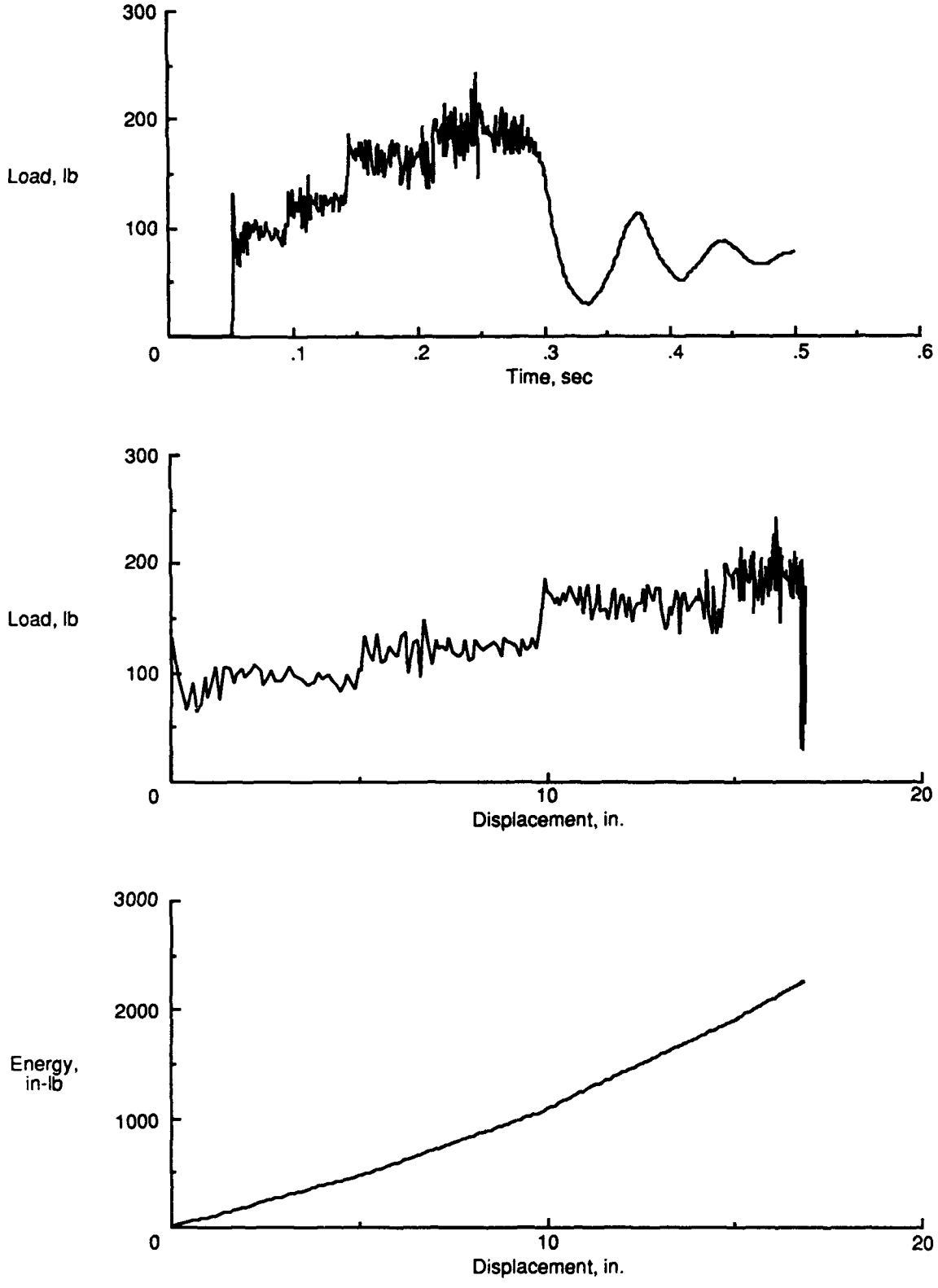

Figure 26. Test 21 specimen type SCTFS.

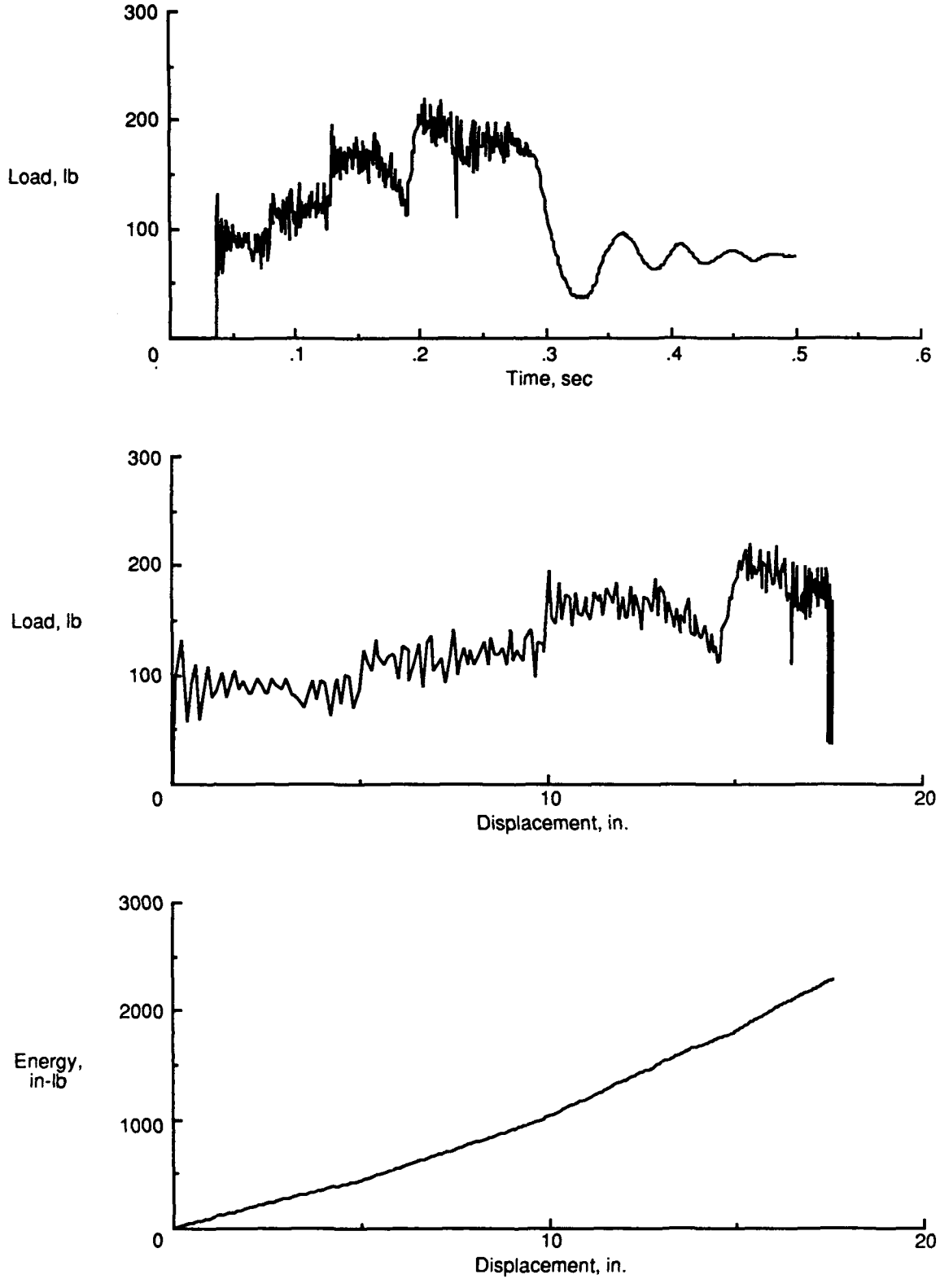

Figure 27. Test 22 specimen type SCTFS.

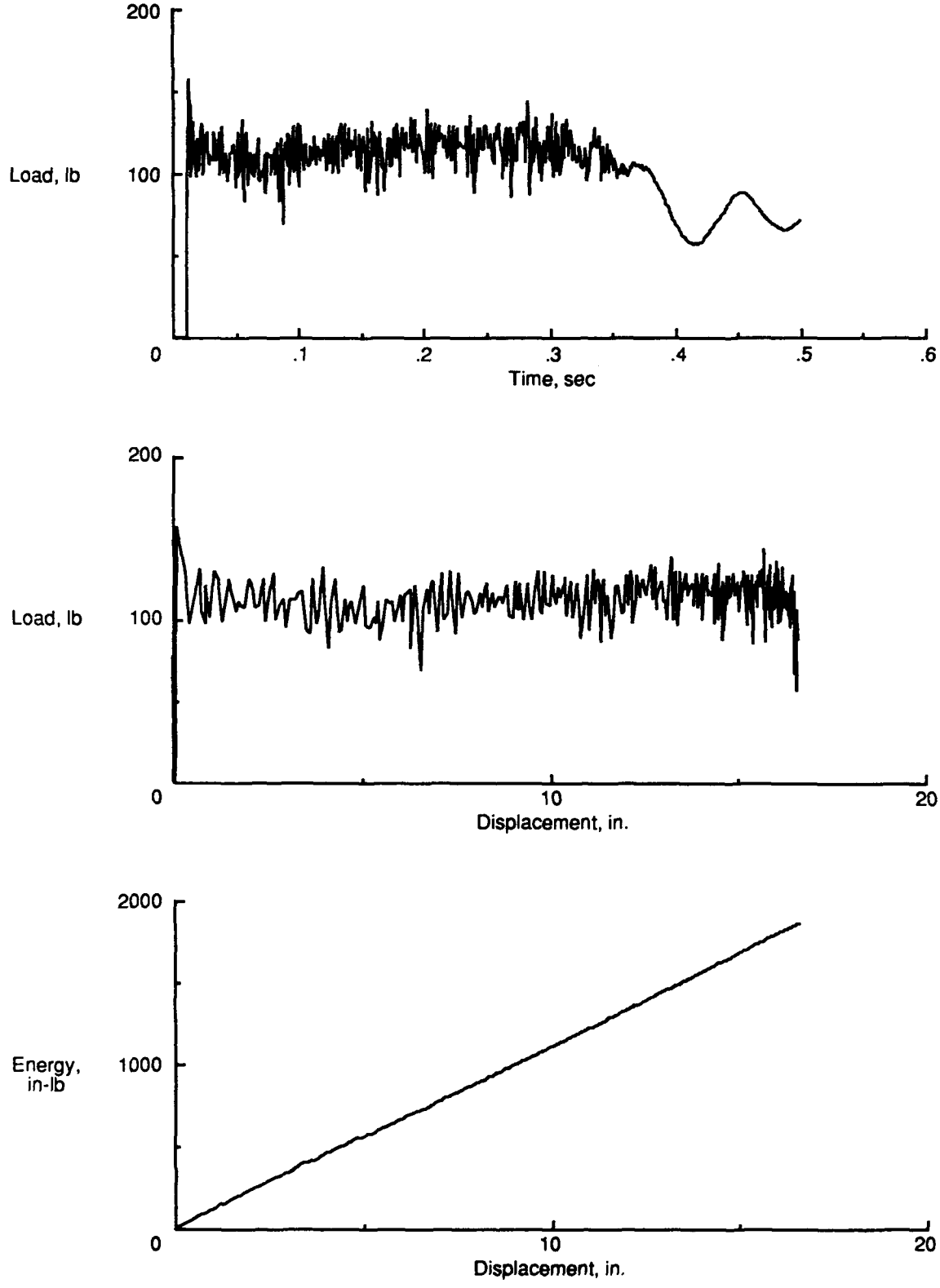

Figure 28. Test 23 specimen type SCTF.

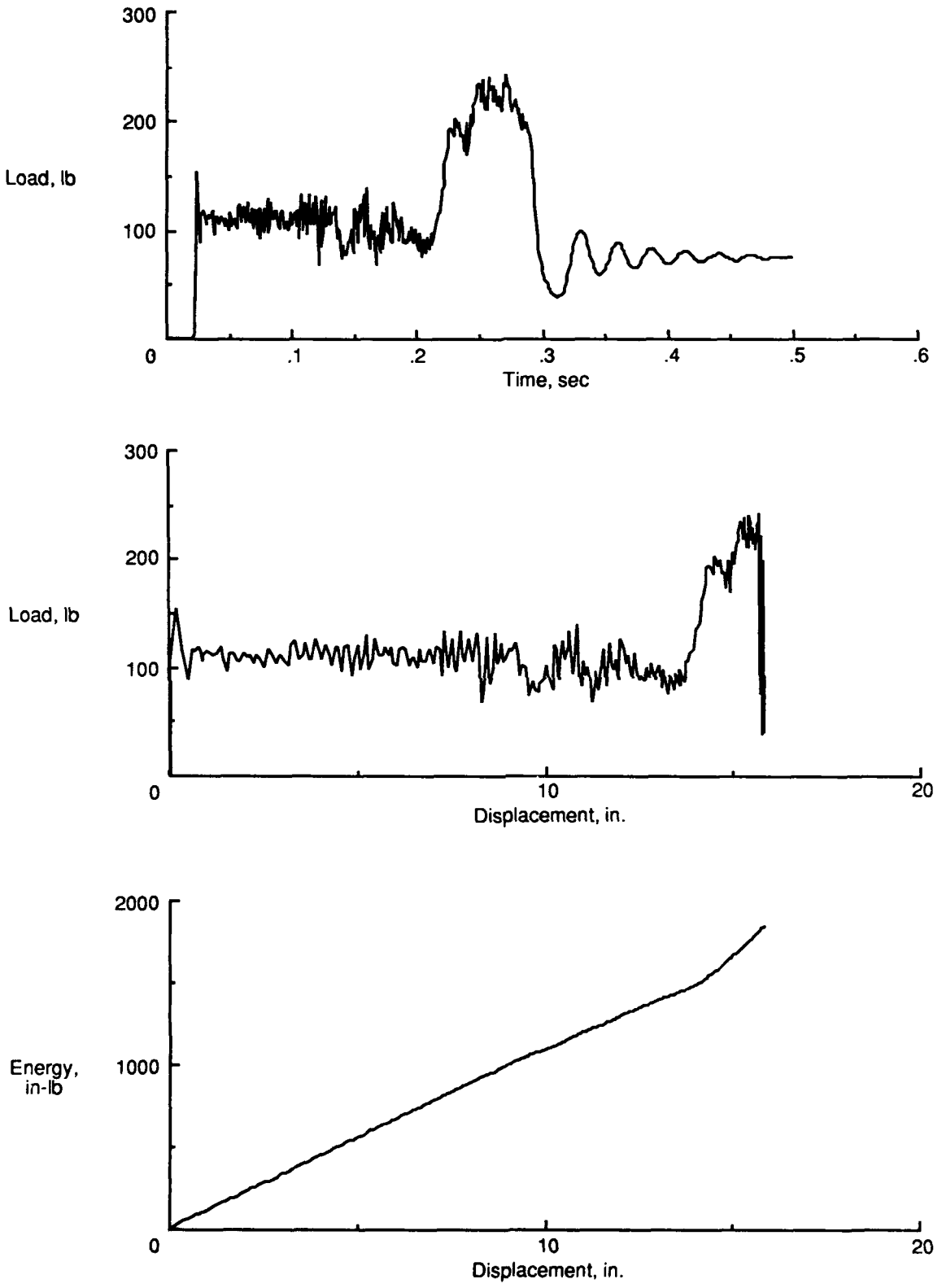

Figure 29. Test 24 specimen type SCTF.

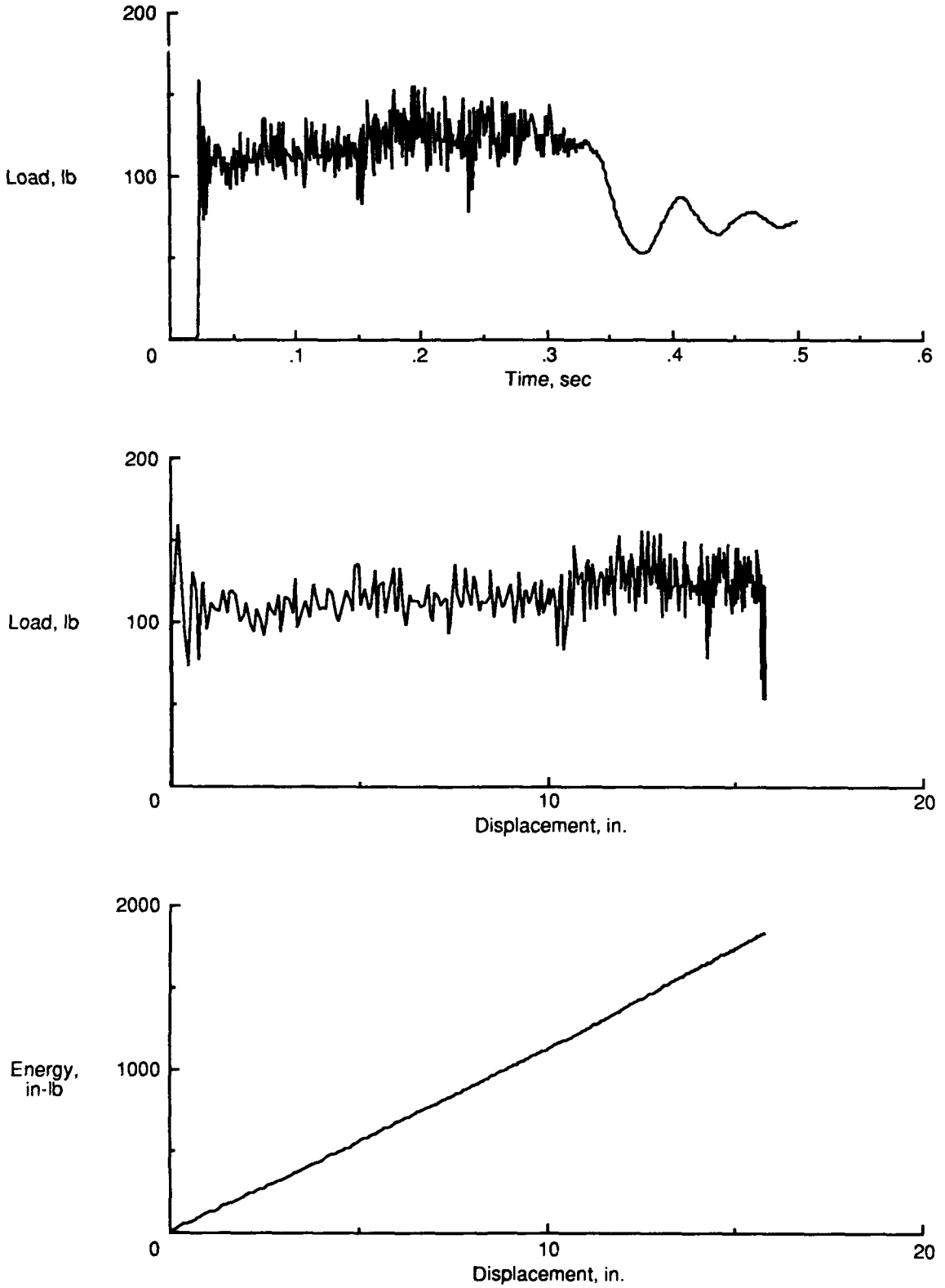

Figure 30. Test 25 specimen type SCTF.

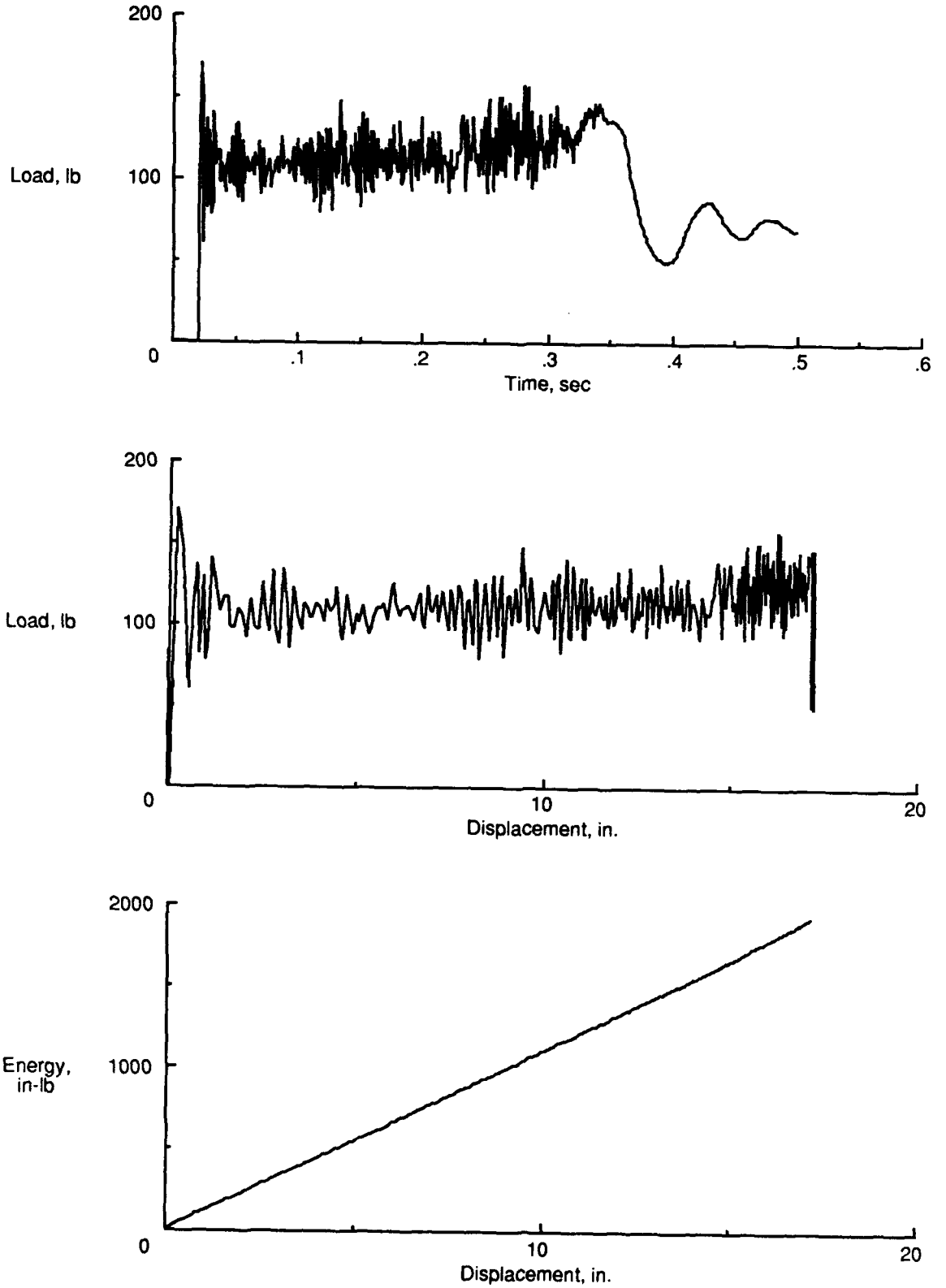

Figure 31. Test 26 specimen type SCTF.

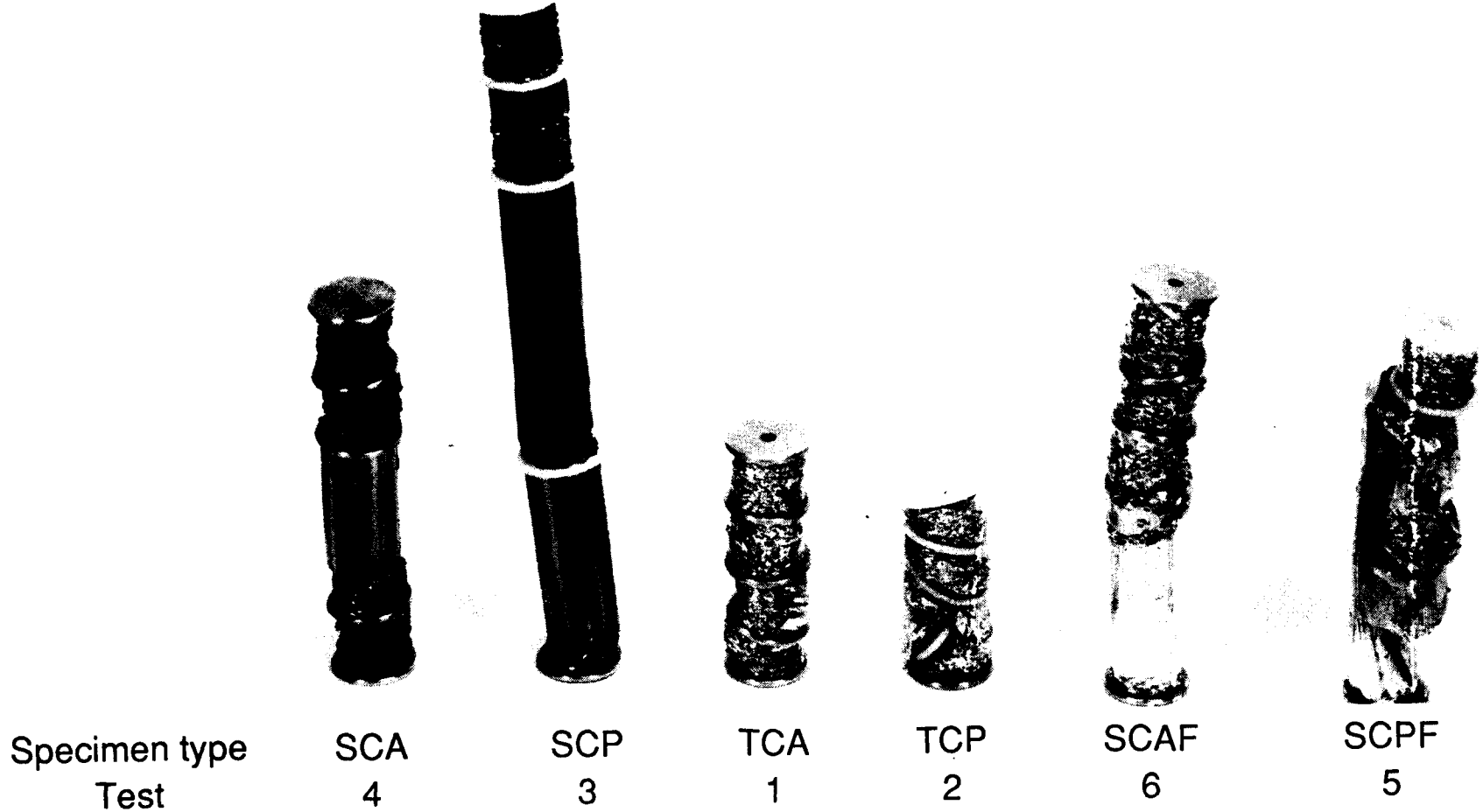

Figure 32. Crushed honeycomb specimens from tests 1 through 6.

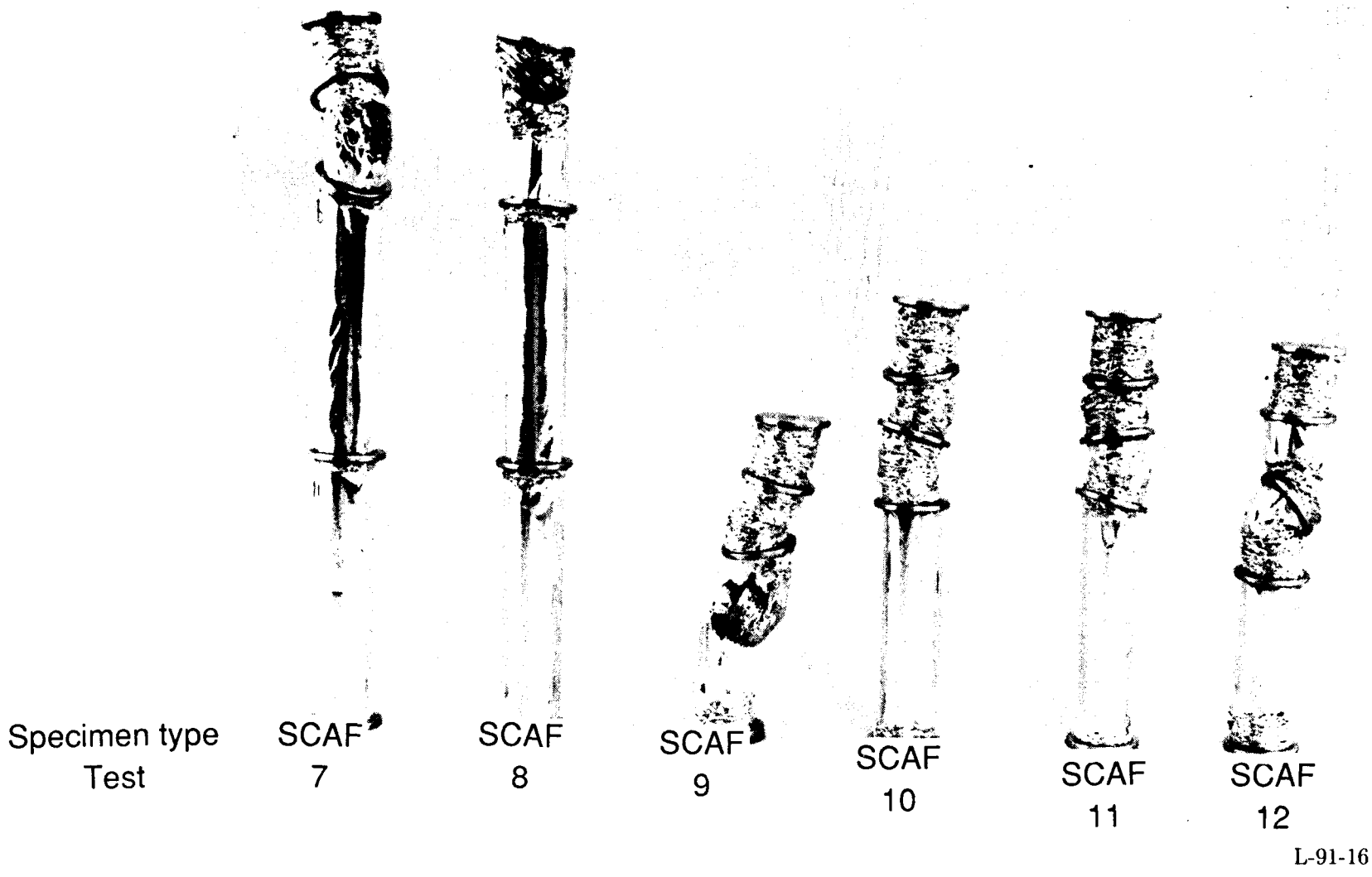

Figure 33. Crushed honeycomb specimens with standard core, aluminum washers, and foil wrap from tests 7 through 12.

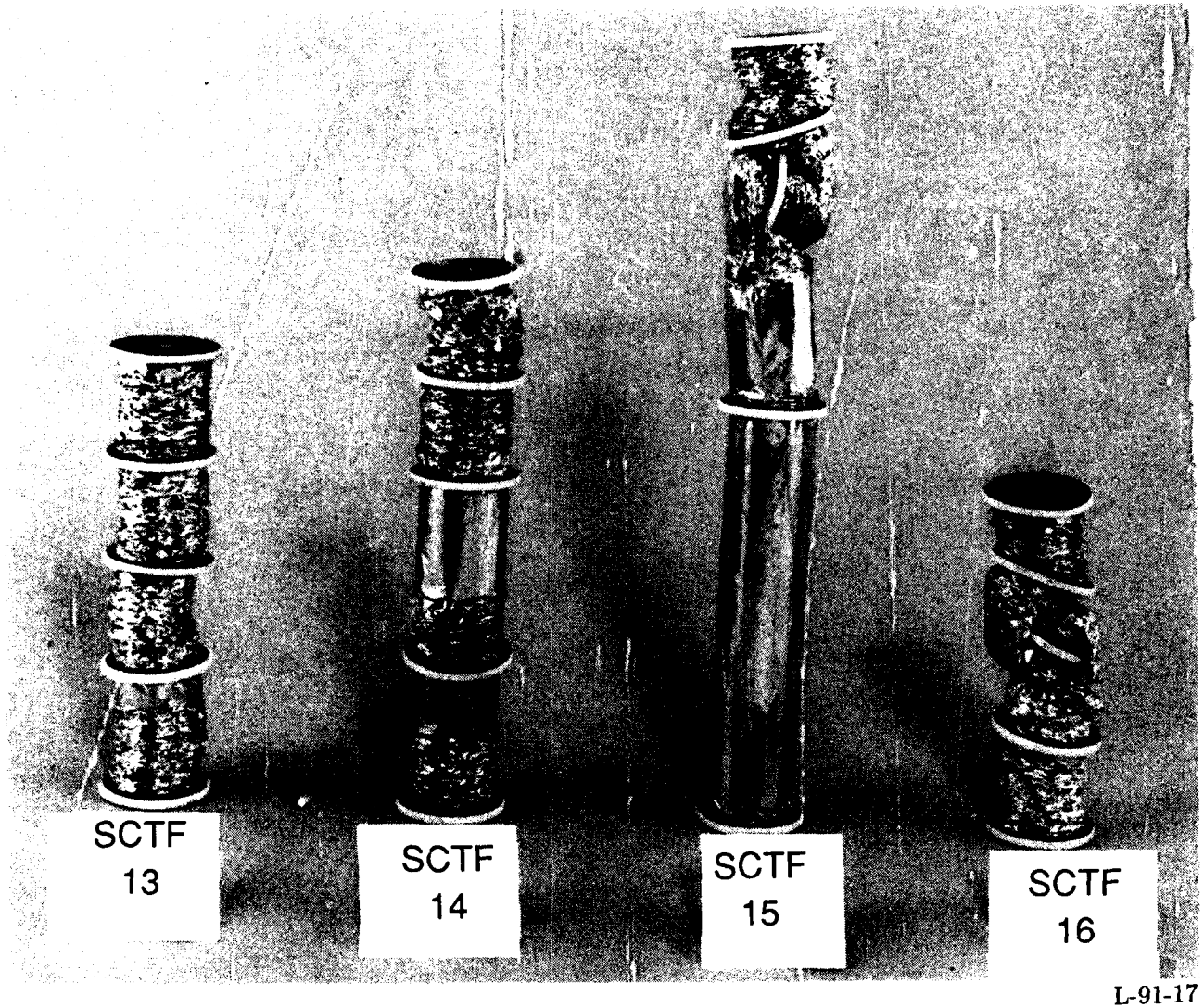

Figure 34. Crushed honeycomb specimens with standard core, Teflon washers, and foil wrap from tests 13 through 16.

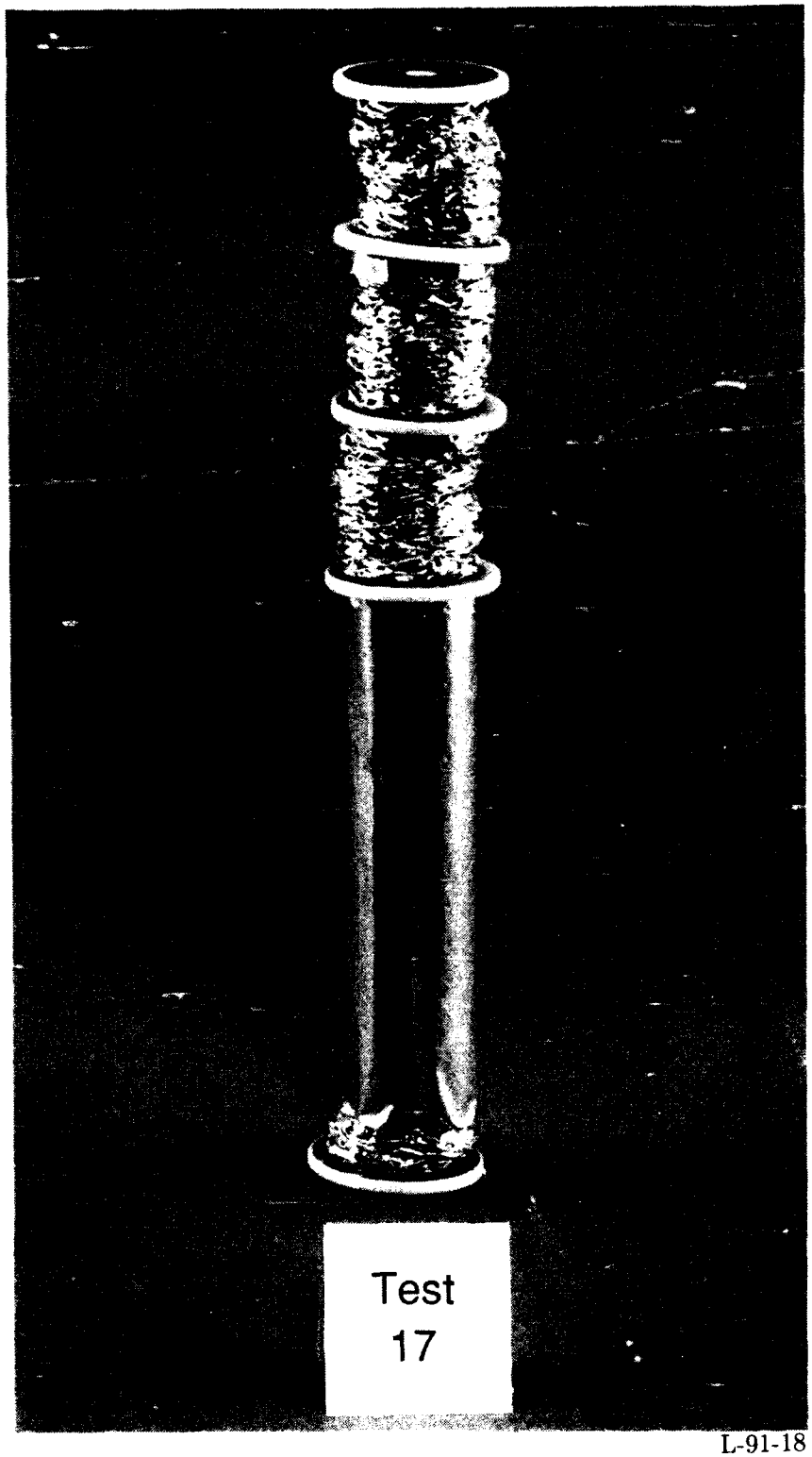

L-91-18

Figure 35. Crushed honeycomb specimen from test 17 conducted with the flight hardware revolver.

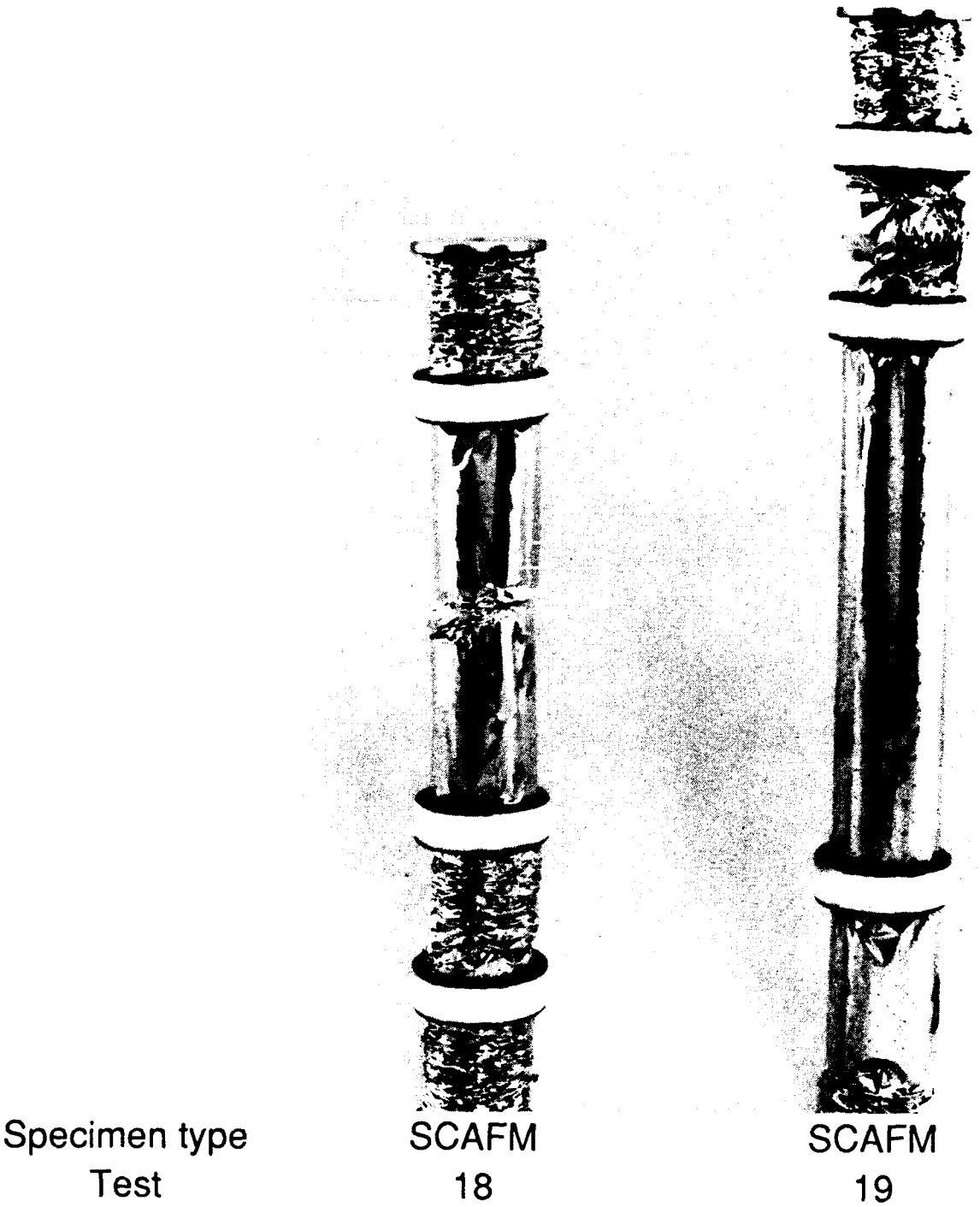

L-91-19

Figure 36. Crushed honeycomb specimens with Teflon plugs from tests 18 and 19.

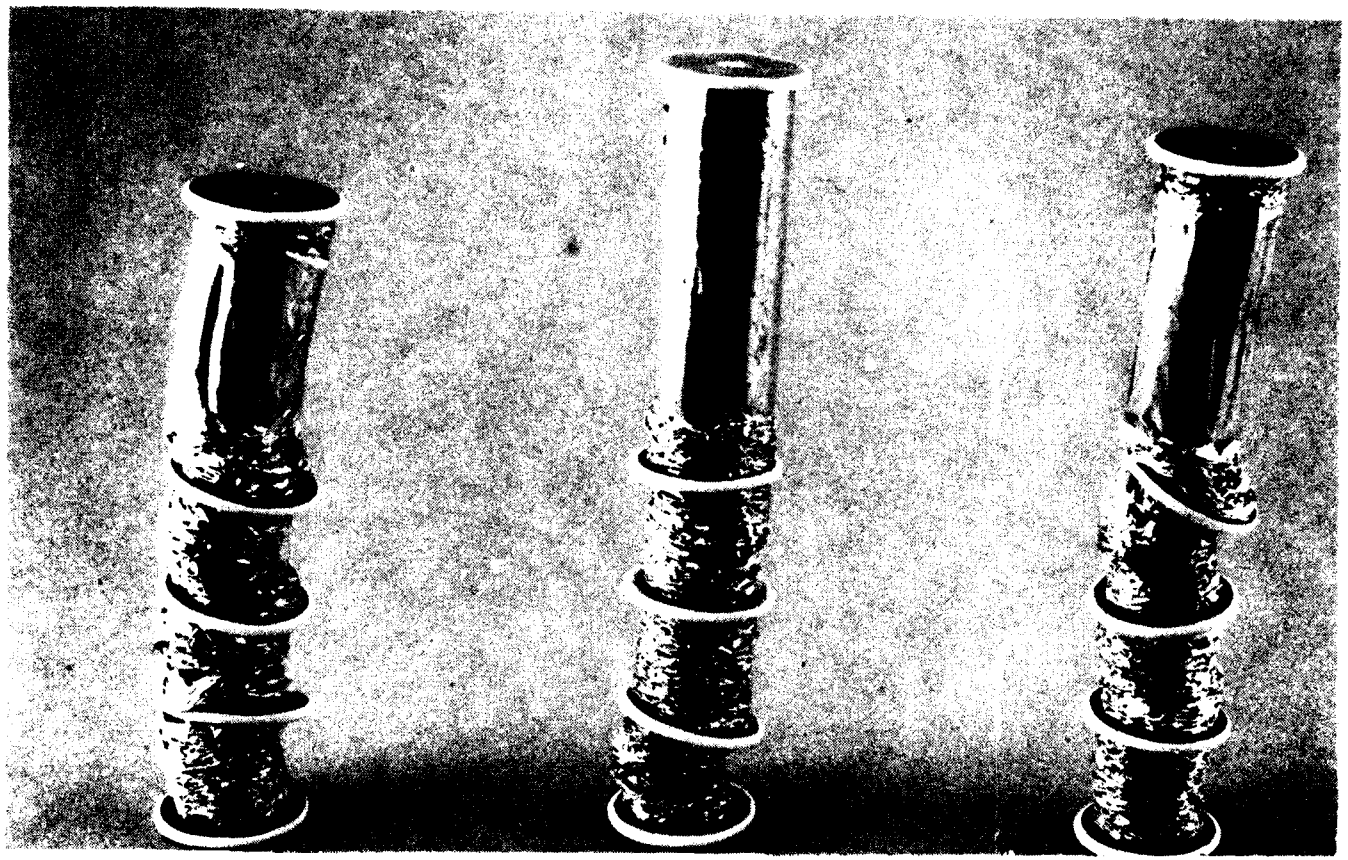

Figure 37. Crushed honeycomb specimens with stepped crush strength from tests 20 through 22. L-91-20

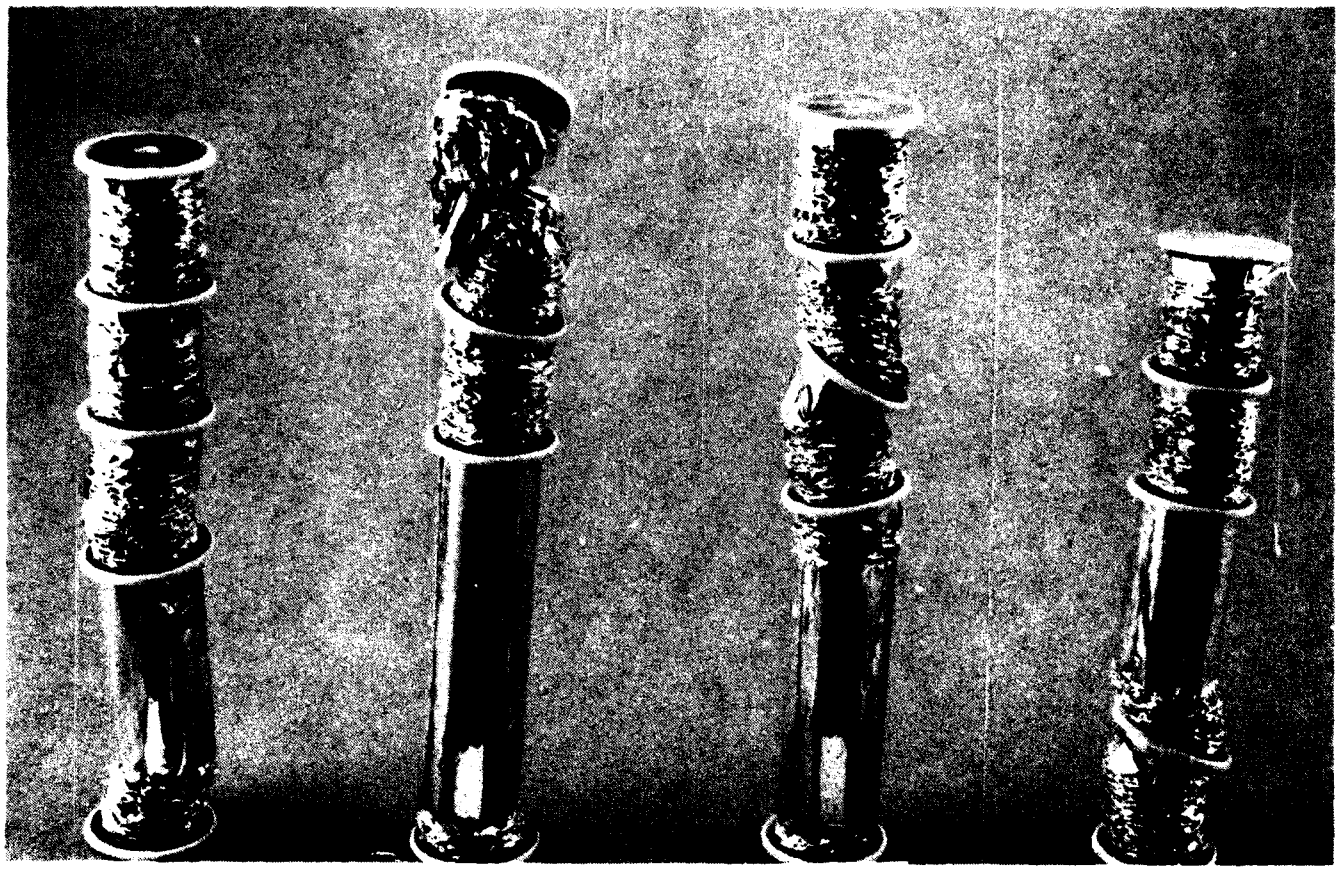

Figure 38. Crushed honeycomb specimens from tests 23 through 26 conducted at a lower impact velocity (8 ft/sec).

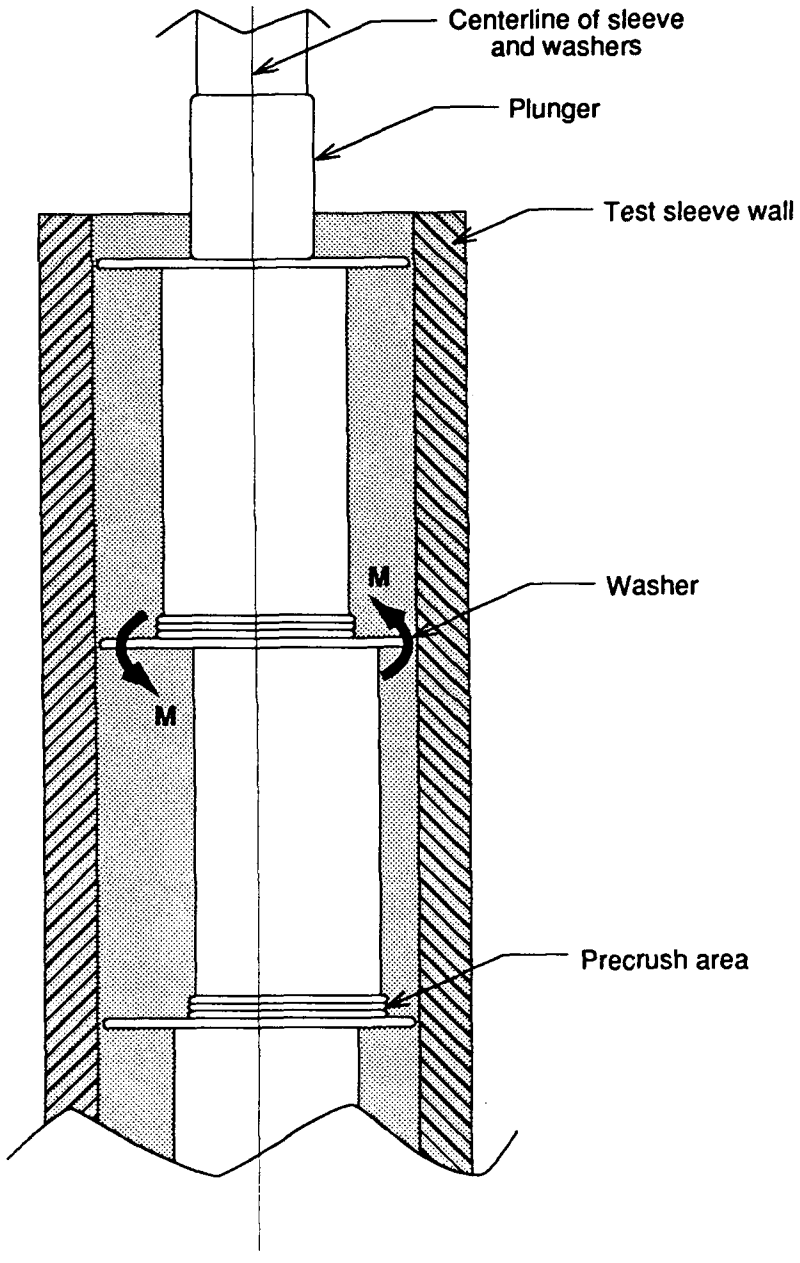

Figure 39. Misalignment of honeycomb segments with centerline of test sleeve. A moment is generated which causes uneven crushing and rotation of the washer. Schematic is not drawn to scale.

NASA
National Aeronautics and Space Administration

Report Documentation Page

1. Report No.	2. Government Accession No.	3. Recipient's Catalog No.
NASA TP-3084 AVSCOM TR-91-B-004		

4. Title and Subtitle	5. Report Date
Determination of Flight Hardware Configuration of Energy-Absorbing Attenuator for Proposed Space Station Crew and Equipment Translation Aid Cart	April 1991
	6. Performing Organization Code
7. Author(s) Edwin L. Fasanella, Karen E. Jackson, Lisa E. Jones, and John E. Teter, Jr.	8. Performing Organization Report No. L-16852
9. Performing Organization Name and Address NASA Langley Research Center and Aerostructures Directorate USAARTA-AVSCOM Hampton, VA 23665-5225	10. Work Unit No. 505-63-01-11
	11. Contract or Grant No.
12. Sponsoring Agency Name and Address National Aeronautics and Space Administration Washington, DC 20546-0001 and U.S. Army Aviation Systems Command St. Louis, MO 63120-1798	13. Type of Report and Period Covered Technical Paper
	14. Army Project No. 1L161102AH45

15. Supplementary Notes

Edwin L. Fasanella: Lockheed Engineering & Sciences Company, Hampton, Virginia.
Karen E. Jackson: Aerostructures Directorate, USAARTA-AVSCOM.
Lisa E. Jones and John E. Teter, Jr.: Langley Research Center, Hampton, Virginia.

16. Abstract

A device incorporating a crushable honeycomb column as the energy-absorbing mechanism was designed as an emergency stopping device for the crew and equipment translation aid (CETA) cart. The CETA cart is designed to transport astronauts along a monorail on the space station. Impact tests were performed to determine which honeycomb design provided a stopping force of 100 lb and energy dissipation of at least 1650 in-lb for 16.5 in. of stroke. A typical honeycomb column consisted of four 5.875-in-long segments of 75-psi honeycomb, separated by 1.5-in-diameter washers. The impact load was provided by a mass which was dropped from a sufficient height to provide one half the equivalent energy of one astronaut plus equipment (500 lb total) moving at 6 ft/sec. Specimen configurations having aluminum, polyethylene, and Teflon washers were tested. Based on the results of impact tests, a honeycomb energy-absorbing column with standard core, foil wrapping, and Teflon washers was chosen for the CETA flight experiment.

17. Key Words (Suggested by Author(s))	18. Distribution Statement
Aluminum honeycomb CETA Energy absorber Impact dynamics	Unclassified—Unlimited Subject Category 39

19. Security Classif. (of this report)	20. Security Classif. (of this page)	21. No. of Pages	22. Price
Unclassified	Unclassified	56	A04

For sale by the National Technical Information Service, Springfield, Virginia 22161-2171